Remote Sensing of Environment 258 (2021) 112368

Contents lists available at ScienceDirect

Remote Sensing of Environment

journal homepage: www.elsevier.com/locate/rse

Spatio-temporal remotely sensed indices identify hotspots of biodiversity conservation concern

Eduarda M.O. Silveira [a,*], Volker C. Radeloff [a], Sebastian Martinuzzi [a], Guillermo J. Martínez Pastur [b], Luis O. Rivera [c], Natalia Politi [c], Leonidas Lizarraga [c], Laura S. Farwell [a], Paul R. Elsen [d], Anna M. Pidgeon [a]

[a] SILVIS Lab, Department of Forest and Wildlife Ecology, University of Wisconsin-Madison, 1630 Linden Drive, Madison, WI 53706, USA
[b] Centro Austral de Investigaciones Científicas (CADIC), Consejo Nacional de Investigaciones Científicas y Técnicas (CONICET), Houssay 200, 9410 Ushuaia, Tierra del Fuego, Argentina
[c] Facultad de Ciencias Agrarias, Universidad Nacional de Jujuy, Consejo Nacional de Investigaciones Científicas y Técnicas (CONICET), Juan Bautista Alberdi 47, Y4600DTA Jujuy, Argentina
[d] Wildlife Conservation Society, Bronx, NY 10460, USA

ARTICLE INFO

Editor: Marie Weiss

Keywords:
Vegetation greenness
Temperature
Phenology
Time series
Image texture
Landsat
MODIS
EVI
LST

ABSTRACT

Over the course of a year, vegetation and temperature have strong phenological and seasonal patterns, respectively, and many species have adapted to these patterns. High inter-annual variability in the phenology of vegetation and in the seasonality of temperature pose a threat for biodiversity. However, areas with high spatial variability likely have higher ecological resilience where inter-annual variability is high, because spatial variability indicates presence of a range of resources, microclimatic refugia, and habitat conditions. The integration of inter-annual and spatial variability is thus important for biodiversity conservation. Areas where spatial variability is low and inter-annual variability is high are likely to limit resilience to disturbance. In contrast, areas of high spatial variability may be high priority candidates for protection. Our goal was to develop spatio-temporal remotely sensed indices to identify hotspots of biodiversity conservation concern. We generated indices that capture the inter-annual and spatial variability of vegetation greenness and land surface temperature and integrated them to identify areas of high, medium, and low biodiversity conservation concern. We applied our method in Argentina (2.8 million km^2), a country with a wide range of climates and biomes. To generate the inter-annual variability indices, we analyzed MODIS Enhanced Vegetation Index (EVI) and Land Surface Temperature (LST) time series from 2001 to 2018, fitted curves to obtain annual phenological and seasonal metrics, and calculated their inter-annual variability. To generate the spatial variability indices, we calculated standard deviation image texture of Landsat 8 EVI and LST. When we integrated our inter-annual and spatial variability indices, areas in the northeast and parts of southern Argentina were the hotspots of highest conservation concern. High inter-annual variability poses a threat in these areas, because spatial variability is low. These are areas where management efforts could be valuable. In contrast, areas in the northwest and central-west are where protection should be strongly considered because the high spatial variability may confer resilience to disturbance, due to the variety of conditions and resources within close proximity. We developed remotely sensed indices to identify hotspots of high and low conservation concern at scales relevant to biodiversity conservation, = which can be used to target management actions in order to minimize biodiversity loss.

1. Introduction

Broad-scale biodiversity patterns are strongly influenced by a host of climatic and environmental factors (Jetz et al., 2019; Pereira et al., 2010; Read et al., 2020; Zarnetske et al., 2019). Among them, climate variability affects many species (MacArthur, 1972), and increasing

* Corresponding author.
E-mail addresses: esilveira@wisc.edu (E.M.O. Silveira), radeloff@wisc.edu (V.C. Radeloff), martinuzzi@wisc.edu (S. Martinuzzi), gpastur@conicet.gov.ar (G.J. Martínez Pastur), natalia.politi@fulbrightmail.org (N. Politi), llizarraga@apn.gob.ar (L. Lizarraga), pelsen@wisc.edu (P.R. Elsen), apidgeon@wisc.edu (A.M. Pidgeon).

https://doi.org/10.1016/j.rse.2021.112368
Received 27 April 2020; Received in revised form 11 February 2021; Accepted 21 February 2021

climate variability due to climate change is a threat for biodiversity (Thuiller et al., 2005; Zhang et al., 2018). Changes in climate can cause changes in the phenology of vegetation greenness (Ma et al., 2013) and in the seasonality of temperature (Mann and Park, 1996). Such changes can lead to phenological mismatches between wildlife species and the resources that they rely on for food, reproduction, and habitat features (Harrington et al., 1999; Menzel et al., 2006; Schwartz et al., 2006). Mismatches result when the timing of regularly repeated phases of life cycles change at different rates in closely interacting species (Renner and Zohner, 2018). Time-sensitive relationships (i.e., availability of food at migration staging areas, or during the breeding period) are altered, modifying the rates of reproduction and survival, causing some populations to decline (Miller-Rushing et al., 2010; Saino et al., 2011). While early or late vegetation phenology can negatively affect species at any time of year (e.g., Allstadt et al., 2015; Beresford et al., 2019; Ferrante et al., 2017), inter-annually unpredictable vegetation phenology is particularly threatening when it occurs during a species' breeding season, which is typically early in the growing season. When species are not able to adjust the timing of their reproduction to track phenological changes (e.g., Glennon et al., 2019; González-Braojos et al., 2017; Socolar et al., 2017), populations decline due to temporal mismatches between the peak of resource needs and of vegetation phenology (Pearce-Higgins et al., 2015; Plard et al., 2014; Saino et al., 2011), posing a threat to biodiversity.

High spatial variability in vegetation greenness and temperature can reduce the threat of biodiversity loss, by bolstering resilience during times of high inter-annual variability (Nyström and Folke, 2001). Resilience to adverse environmental conditions is higher where spatial variability of resources is higher (Peterson et al., 1998; Malika et al., 2009). Ecosystems with high spatial variability provide a range of resources, habitat conditions, and microclimatic refugia (Oliver et al., 2010) within a small area. Such conditions can enhance species survival during periods of pronounced climate extremes (Thuiller et al., 2005), and maintain ecological processes during periods of environmental stress (Loreau et al., 2001; Tilman, 1999). The reason is that spatial variability in vegetation greenness is associated with asynchrony of both plants and plant-dependent resources that are in close proximity (Farwell et al., 2020), and high spatial variability in temperature may provide thermal refugia (Elsen et al., 2020, 2021). Indeed, spatial variability in vegetation shapes biodiversity patterns and ecosystem stability at fine scales by way of vegetation species diversity and the associated range of nutritional and structural attributes (Levin et al., 2007), and at broad scales through diversity of land cover types. Ecosystems that have both high spatial variability and high biodiversity are more ecological resilient (Peterson et al., 1998), have higher species survival, and recover more quickly during adverse conditions (Oliver et al., 2010, 2015). Here, we adopt the definition of ecological resilience as a measure of the amount of change needed to change an ecosystem from one set of processes and structures to a different set of processes and structures (Angeler and Allen, 2016; Folke et al., 2004; Holling, 1973).

Similarly, high spatial variability in land surface temperature offers a variety of microclimates in close proximity, which can provide thermal refugia (Keppel et al., 2012) by reducing exposure to extreme temperatures (Elsen et al., 2020, 2021). Especially for non-mobile species, spatial variability in vegetation greenness and temperature makes it more likely that at least some individuals can persist during extreme events (Keppel et al., 2012). High spatial variability only provides refugia when that spatial variability occurs within a given species' suitable habitat. In contrast, fragmentation of naturally contiguous habitat can cause high spatial variability in vegetation greenness or temperature but that would likely have negative consequences for biodiversity (Fahrig, 2003; Fletcher et al., 2018). However, spatially variable landscapes with limited amounts of human modifications can enhance resilience to the threat that high inter-annual variability in vegetation phenology poses for biodiversity and can reduce the likelihood of a temporal mismatch between animal's needs and available resources (Oliver et al., 2015; Robinson et al., 2016; Virah-sawmy et al., 2009).

Inter-annual variability in the phenology of vegetation greenness and in the seasonality of temperature can be effectively captured from time series of satellite-based vegetation indices (Hmimina et al., 2013; Jin and Eklundh, 2014) and thermal infrared data (Albright et al., 2011; Hengl et al., 2012). Such time-serie s are particularly powerful when derived from coarse-resolution sensors such as the Moderate-Resolution Imaging Spectroradiometer (MODIS) because of their high temporal frequency. Phenology metrics, such as the start of the growing season, derived from time series of the Enhanced Vegetation Index (EVI) capture intra-annual variability of vegetation greenness (Deng et al., 2019; Hu et al., 2019) because EVI is correlated with the greenness of the vegetation canopy, which is related to photosynthetic activity and leaf area (Huete et al., 2002). One advantage of the EVI over other vegetation indices is that it is less sensitive to saturation over dense vegetation due to lower dependence on the red band (Huete et al., 1999). Furthermore, the inclusion of the blue band in EVI minimizes soil and atmospheric effects, resulting in better greenness estimates than the Normalized Difference Vegetation Index (NDVI; Matsushita et al., 2007).

Land surface phenology captures seasonal patterns in the vegetation on the land surface captured by satellite sensors (de Beurs and Henebry, 2005). The reflectance properties of vegetation vary seasonally in relation to vegetation phenology, however, because vegetation indices provide measures of vegetation productivity and do not directly record specific phenological events, such as flowering (Atkinson et al., 2012), they are at best proxies of vegetation phenology (Ganguly et al., 2010; Liu et al., 2016; Wu et al., 2014), which is a common limitation of phenology estimates based on remotely-sensed data (de Beurs and Henebry, 2005, 2010). Reasons that vegetation phenology differs from greenness phenology in satellite imagery include the mixing of signal and background, especially in coarse spatial resolution satellite images, limited sensitivity of vegetation indices during budburst, the saturation of vegetation indices at peak greenness, and others which is why greenness is related, but not identical, to vegetation phenology (Morisette et al., 2009; White et al., 2009; White and Nemani, 2006).

Satellite sensors also provide actual measurements of Land Surface Temperature (LST) at fine resolution for large areas, which is an advantage compared to interpolated temperature data from meteorological stations, which can introduce errors and bias (Behnke et al., 2016). While measures of LST also contain errors and biases (Barsi et al., 2014), the Landsat's Thermal Infrared Sensor (TIRS) data represents the highest-resolution source of remotely sensed thermal data with global coverage. LST from satellite data indicates hotness or coldness of the earth surface and is based on mean effective radiative temperature of various canopy and soil surfaces (García-álvarez et al., 2019). MODIS daily LST products obtained from thermal infrared data are available from 2000 to the present (Lu et al., 2018), thus enabling the study of the seasonality of LST and its variability among years over almost two decades.

Spatial variability in vegetation greenness or land surface temperature can be captured by calculating image texture, i.e., statistical measures of the variability among pixels in a moving window (Haralick et al., 1973), and image textures are effective measures of habitat suitability for wildlife (Bellis et al., 2008; Farwell et al., 2020; Wood et al., 2013). Landsat imagery, with its 30-m resolution, can capture both spatial variability in greenness when applied to Landsat-derived vegetation indices (Farwell et al., 2020, 2021; Lu and Batistella, 2005), and spatial variability in temperature when applied to thermal bands (Elsen et al., 2020, 2021). Texture measures reflect both vegetation heterogeneity and vegetation patterns (Ge et al., 2006). For example, image texture is correlated with foliage-height diversity and horizontal vegetation structure (26-60% of the variation), and captures within-class variability that categorical land cover classifications miss (Wood et al., 2012). Among the different image texture variables (Haralick et al.,

1973), the standard deviation of pixel values within a moving window characterizes landscape heterogeneity well. For example, the standard deviation of vegetation indices explains up to 43% of the variability in leaf area index in northern deciduous and mixed wood forests in Canada (Wulder et al., 1998). The standard deviation of 30-m resolution EVI data has a positive relationship with overall bird species richness across the conterminous United States (Farwell et al., 2020). In addition, the standard deviation of winter land surface temperature is positively related with the variability of resident bird richness across the conterminous USA explaining 37% of the variability (Elsen et al., 2020). These relationships suggest that image texture provide proxy measures of vegetation structure and temperature patterns that are relevant for biodiversity.

Identifying the spatio-temporal patterns of vegetation greenness and land surface temperature is both scientifically interesting and important for biodiversity conservation efforts. In many cases, conservation requires prioritization, i.e., identification of the areas where conservation investments make the biggest difference (Wilson et al., 2006), where new protected areas are most valuable (Possingham et al., 2006; Venter et al., 2014), or where conservation actions should be targeted (Hmielowski et al., 2015). Maps of spatio-temporal variability in vegetation greenness and land surface temperature can potentially inform such prioritizations and decision-making. For example, areas with high inter-annual variability in the phenology of vegetation or in the seasonality of temperature may require management actions that enhance spatial variability in vegetation greenness and land surface temperature to enhance resilience to biodiversity loss from high inter-annual variability. In contrast, areas where spatial variability is high may be of high priority for protection because this is where species are more likely to persist if inter-annual variability increases due to climate change.

Our goal was to develop spatio-temporal remotely sensed indices to identify hotspots of biodiversity conservation concern due to threats from high inter-annual variability. Our objectives were to: (1) generate remotely sensed indices that capture inter-annual and spatial variability in the phenology of vegetation greenness and in the seasonality of land surface temperature; and (2) integrate the inter-annual and spatial variability indices to identify areas of high, medium, and low biodiversity conservation concern.

2. Methods

2.1. Study area

Our study area is the country of Argentina (2.8 million km^2) located in South America, between 20°S and 60°S latitudes, and 50°W and 80°W longitudes (Fig. 1a), excluding the Malvinas/Falkland archipelago and southern Atlantic islands. The climates of Argentina are diverse due to the wide latitudinal and altitudinal gradients and include tropical, arid, temperate, cold, and polar climates (Köppen et al., 2011). The northern part of the country is characterized by hot, humid, rainy summers and mild winters, while the southern part has a dry climate with warm summers and cold winters. Mean annual precipitation (MAP) ranges

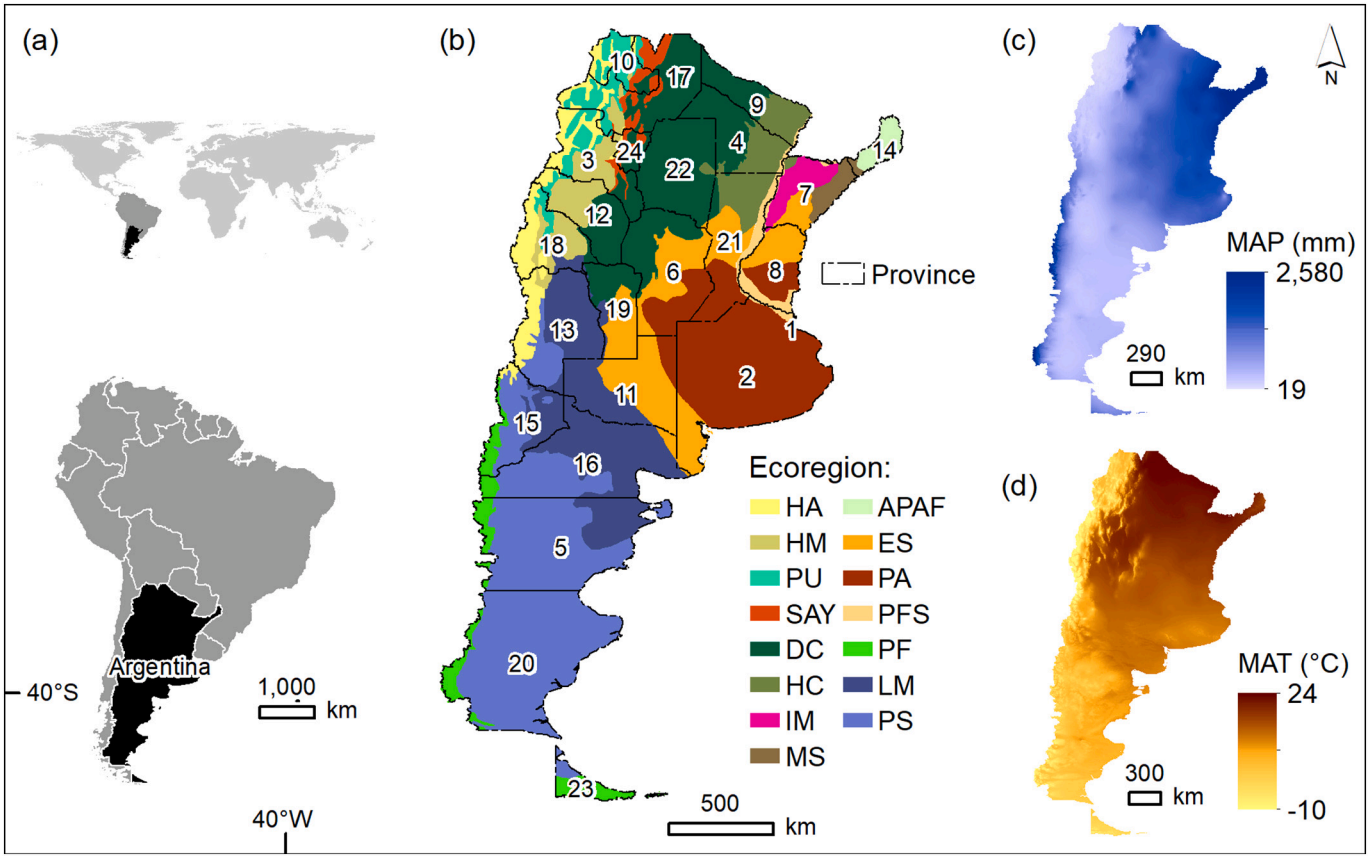

Fig. 1. Location of Argentina within South America (a), and bioclimatic characteristics of Argentina, including: (b) administrative provinces (black lines): 1 – Autonomous city of Buenos Aires, 2 – Buenos Aires, 3 – Catamarca, 4 – Chaco, 5 – Chubut, 6 – Córdoba, 7 – Corrientes, 8 – Entre Rios, 9 – Formosa, 10 – Jujuy, 11 – La Pampa, 12 – La Roja, 13 – Mendoza, 14 – Misiones, 15 – Neuquén, 16 – Rio Negro, 17 – Salta, 18 – San Juan, 19 – San Luis, 20 – Santa Cruz, 21 – Santa Fé, 22 – Santiago del Estero, 23 – Tierra del Fuego, 24 – Tucumán; and ecoregion boundaries (colored polygons): High Andes (HA), High Monte (HM), Puna (PU), Southern Andean Yungas (SAY), Dry Chaco (DC), Humid Chaco (HC), Ibera marshes (IM), Mesopotamian savanna (MS), Alto Parana Atlantic forests (APAF), Espinal (ES), Pampa (PA), Parana flooded savanna (PFS), Patagonian forests (PF), Low Monte (LM), Patagonian steppe (PS) (Burkart et al., 1999); (c) mean annual precipitation (MAP, mm.yr^{-1}); and (d) mean annual temperature, (MAT, °C).

from 19 to 2,580 mm, and mean annual temperature (MAT) from -10°C to 24°C (Fig. 1c–d). Temperatures decrease from north to south and there is also a gradient in temperature and precipitation from west to east due to topographic contrast between the mountainous western and flat eastern parts of the country (Barros et al., 2015).

Argentina has eighteen ecoregions (Burkart et al., 1999) comprising mountains, lowlands, cold and warm regions, and dry and wet forests (Barros et al., 2015); fifteen ecoregions are continental, two are marine, and one is Antarctic. We performed the analysis at a nation-wide scale (country of Argentina) and at two finer scales, i.e., for each of the continental ecoregions (15) and provinces (23) of Argentina (Fig. 1b). We intersected boundaries of ecoregions and provinces, which resulted in 96 polygons and helped us to identify hotspots of high and low conservation concern in greater detail. We chose Argentina's ecoregions as a scale of analysis because they are relatively homogeneous in terms of geomorphological, hydrological, soil, vegetation and climate characteristics (Burkart et al., 1999). The ecoregions are also important for environmental assessments and management, and allow comparison of different areas (Loveland and Merchant, 2004). Provinces are administrative regions, and many land use and conservation decisions, including delineation of forest land use zones, are made at the province level. While ecoregional analyses are more ecologically relevant, provinces are the unit at which the government conducts conservation and management, and thus, intersecting ecoregions and provinces provides valuable information that is both ecologically relevant and suitable for defining conservation and management priorities.

In 2007, Argentina implemented the 'Forest Law' (N. 26 331) to promote more sustainable forest management (Martinuzzi et al., 2018; Seghezzo et al., 2011). Unfortunately, the resulting land use plans did not incorporate biodiversity information explicitly. However, these plans are updated every five years, and inclusion of biodiversity and habitat data can greatly improve the plans (Martinuzzi et al., 2018). Thus, knowledge of patterns of inter-annual and spatial variability of vegetation greenness and land surface temperature can help to identify those areas where many species may have difficulty persisting if climate becomes more extreme, as well as areas where climate extremes would likely have less of an effect, and thus where biodiversity is more likely to persist.

Table 1
Potential integrations of inter-annual and spatial variability in vegetation greenness and land surface temperature, and the level of conservation concern for each integration.

		Spatial variability	
		High	Low
Inter-annual variability	High	*Medium conservation concern* from phenological and seasonal variations because high inter-annual variability poses a high level of threat, but high spatial variability of vegetation greenness and temperature means that resilience is high	*Highest conservation concern* from phenological and seasonal variations because high inter-annual variability poses a high level of threat, and low spatial variability of vegetation greenness and temperature means that resilience is low
	Low	*Lowest conservation concern* from phenological and seasonal variations because low inter-annual variability entails a low level of threat, and high spatial variability in vegetation greenness and temperature means that resilience is high	*Medium conservation concern* from phenological and seasonal variations because low inter-annual variability entails a low level of threat, but low spatial variability in vegetation greenness and temperature means that resilience is low

2.2. Assumptions and definitions

We based our analyses on three assumptions (Table 1). First, we assumed that high inter-annual variability in the phenology of vegetation greenness and in the seasonality of land surface temperature is a threat for biodiversity. If inter-annual variability is high, then there is a higher likelihood that physiological tolerances of species are exceeded and that there are mismatches between animal requirements and resource availability. Many plants and animals have phenological relationships, that is they synchronize their seasonal timing of life events. Mismatches in the timing of such events, can entail, for example, food limitations when wildlife species miss the annual peak in food abundance, which may affect reproduction or survival (Menzel et al., 2006; Reed et al., 2013). Thus, high inter-annual variability in the phenology of vegetation greenness or in the seasonality of land surface temperature can exceed the rate at which organisms are able to adapt, disrupting the synchrony of ecological interactions, and pose a threat for biodiversity (Harrington et al., 1999; Menzel et al., 2006; Thackeray et al., 2010).

Second, we assumed that high spatial variability in vegetation greenness and land surface temperature enhance resilience to high inter-annual variability. In general, ecological communities and species' populations differ in how they respond to perturbations based on how resilient they are (Angeler and Allen, 2016). High spatial variability increases resilience (Malika et al., 2009), because areas with higher spatial variability have higher species' survival rates during rapid climatic changes than areas with low spatial variability. In addition, higher biodiversity can improve ecological resilience and resistance because it allows the community to either withstand or recover faster from disturbances (Oliver et al., 2015; Angeler and Allen, 2016). Thus, high spatial variability of biotic and abiotic conditions can bolster resilience (Thuiller et al., 2005; Nyström and Folke, 2001), is associated with higher species richness (Elsen et al., 2020; Farwell et al., 2020), and increases the likelihood for renewal and reorganization after disturbance (Folke et al., 2004). This is why we assume that biodiversity benefits from high spatial variability in vegetation greenness and land surface temperature in areas that are fairly natural, because such spatial variability provides a variety of resources in close proximity, and increases the likelihood that suitable conditions are available during times of extremes. Accordingly, we assumed that such conditions enhances the resilience to high inter-annual variability.

Third, the areas of highest conservation concern due to the spatio-temporal patterns are those where inter-annual variability in phenology is high, which poses a high level of threat, and spatial variability of vegetation greenness and land surface temperature is low, which means that ecological resilience is likely lower (Table 1). A medium level of conservation concern occurs when both types of variability are high or both are low. The lowest level of conservation concern occurs where inter-annual variability is low, and spatial variability is high, i.e., where threat is low, and resilience is likely high.

2.3. Inter-annual variability analysis

We characterized inter-annual variability in the phenology of vegetation greenness and in the seasonality of land surface temperature based on EVI and LST time series from 2001 to 2018 as captured by the MODIS sensor on board of Terra. For inter-annual variability in the phenology of vegetation greenness, we analyzed MODIS 16-days Vegetation Indices (MOD13Q1-collection 6; 250-m resolution). For inter-annual variability in the seasonality of land surface temperature, we analyzed MODIS 8-day LST (MOD11A2-Collection 6; 1-km resolution). We acquired images from Google Earth Engine, and selected only cloud-free data of optimal quality according to the MODIS Quality Assurance flags. Using TIMESAT 3.3 software (Jönsson and Eklundh, 2004), we modeled the 18-year EVI and LST time series using an iterative median filter followed by an adaptive Savitzky-Golay filter, which uses local polynomial functions in the fitting (Savitzky and Golay, 1964). Based on

the resulting curves, we calculated three phenology (when referring to vegetation greenness) and three seasonal (when referring to land surface temperature) metrics for each year of analysis, i.e. the start date, end date, and length of the growing season for EVI and LST (Table 2). Start of the growing season, in spring, was defined as the day of the year when EVI is >25% of the annual maximum, and end of the growing season, in autumn, when EVI is <25% of the annual maximum (Blundo et al., 2018; Ren et al., 2017; Van Leeuwen et al., 2013).

To quantify inter-annual variability, we computed the coefficient of variation (CV) among years for each of the six metrics (Table 2). Because CV is a measure of variability over time, the index reflects phenological timing differences at the pixel level for any land cover type. However, within land cover classes some areas are more uniform in start of the growing season (SOS) among years, due, for example, to low topographic variation and low canopy species richness, while in other areas the CV of SOS may be higher due to, for example, to interactions among canopy species numbers, temperature conditions, and topography (Misra et al., 2018; Xia et al., 2019). We calculated the CVs only for pixels for which we could obtain the phenological or seasonal metrics for at least 15 of the 18 years of our analysis. No-data values represent missing data or areas where we had less than 15 years of metrics.

We suspected that the phenological and seasonal metrics would be correlated, and calculated Pearson's correlation coefficients (r) among the three greenness and the three land surface temperature temporal variability indices, respectively, to decide if it was meaningful to retain all indices for further analyses. We performed the Pearson's correlation analysis based on 5,000 points randomly distributed over the study area. Because correlations were strong, we conducted a principal component analysis (PCA) for greenness and one for temperature (Jolliffe and Cadima, 2016). The first principal component of the PCA captures the greatest variance, the second component captures the maximum amount of variance not described by the first, and so forth. However, principal components are by definition derived from multiple variables, and that can make it difficult to interpret their values, which is why we selected the seasonal metric that was most strongly correlated with the first principal component for further analysis rather than the first principal component itself.

Table 2
Phenology and seasonality metrics and inter-annual variability indices of vegetation greenness and land surface temperature calculated from the enhanced vegetation index (EVI) and land surface temperature (LST) MODIS time series from 2001 to 2018.

Phenology and seasonality metrics	Description	Inter-annual variability Index	Description
EVI_SOS	Start of the growing Season (SOS) calculated from the EVI time series defined as the first day of year (DOY) in spring when EVI is >25% of the annual maximum.	CV_EVI_SOS	Coefficient of variation of EVI_SOS
EVI_EOS	End of the growing Season (EOS) calculated from the EVI time series defined as the first DOY in autumn when EVI is <25% of the annual maximum.	CV_EVI_EOS	Coefficient of variation EVI_EOS
EVI_LOS	Length of the growing Season (LOS) defined as the number of days between the start and end dates.	CV_EVI_LOS	Coefficient of variation of the EVI_LOS
LST_SOS	The DOY in spring when LST is >25% of the annual maximum.	CV_LST_SOS	Coefficient of variation of LST_SOS
LST_EOS	The DOY in autumn when LST is <25% of the annual maximum.	CV_LST_EOS	Coefficient of variation of LST_EOS
LST_LOS	The number of days between LST_SOS and LST_EOS.	CV_LST_LOS	Coefficient of variation of LST_LOS

2.4. Spatial analysis

We characterized spatial variability in vegetation greenness and in land surface temperature by calculating the standard deviation image texture (Haralick et al., 1973) of EVI and LST images from Landsat imagery, which we processed in Google Earth Engine. We chose standard deviation, rather than a measure that accounts for differences in the mean, such as the coefficient of variation, because the EVI can have a very low mean in areas with sparse vegetation, and when that occurs, the values for the coefficient of variation become extremely high.

We calculated spatial variability in vegetation greenness based on the EVI from Landsat 8 Surface Reflectance Tier 1 bands 2, 3 and 4. First, we masked pixels covered by clouds, shadows, or water based on the Quality Assurance flags and a static water mask derived from Landsat imagery (Hansen et al., 2013). Second, we generated a composite image by calculating the 90th percentiles of EVI values from all years from 2013 to 2018 during all seasons. This way, we characterized peak of vegetation greenness while excluding erroneously high EVI values (Farwell et al., 2020). Third, to obtain our vegetation greenness spatial variability index, we applied an 11 × 11 pixel moving window to calculate the standard deviation of the composite EVI 90th percentile image. Thus, the central pixel within the moving window was assigned a standard deviation value based on the EVI 90th percentile of the neighboring pixels.

For land surface temperature spatial variability, we assessed LST from Band 10 of the thermal infrared sensor (TIRS) of Landsat 8, which USGS provides statistically downscaled at 30-m resolution. We analyzed only data from Band 10 because Landsat 8's band 11 has a larger bias and more scatter (Barsi et al., 2014). We first selected all the images collected from 2013 to 2018 during the warmest third of the year (i.e., from November to February, hereafter 'summer') and the coldest third of the year (i.e., from May to August, hereafter, 'winter'). Summer was composed of median values from November to February, and winter was composed of median values from May to August, from all the years combined (2013, 2014, 2015, 2016, 2017 and 2018). By analyzing median values instead of the mean, we minimized the effects of extremes and spuriously high/low values in the temperature data, and minimized gaps due to cloud contamination (Elsen et al., 2020). We calculated standard deviation within an 11 × 11 pixel moving window for summer and winter based on the median composite images for summer and winter separately. We measured the standard deviation for summer and winter separately to capture thermal variability of extremes during these seasons because both hot and cold temperatures extremes can influence biodiversity patterns (Clarke and Gaston, 2006; Elsen et al., 2020).

Ultimately, to identify spatial variability in land surface temperature for both hot and cold temperatures, we generated one land surface temperature variability index by combining data from summer and winter (Fig. S1). To do so, we classified the summer and winter standard deviation images into five quantile classes, ranging from 1 (low standard deviation values, low variability) to 5 (high standard deviation values, high variability) (Fig. S1, 2a,b). We combined the two classified images into all possible combinations, resulting in 25 classes. We summarized the values of each combination resulting in values from 2 to 10 (Fig. S1, 3). In a final step, we classified areas where spatial variability in both summer and winter are high as high spatial variability (sum ≥7) while low spatial variability represents areas where spatial variability in both summer and winter was low (sum ranging from 2 to 6; Fig. S1, 4).

We chose our window size for both ecological and methodological reasons. Ecologically, a 330-m window, given Landsat's 30-m window size is small enough to assume that most species can reach a refugia within that area. Methodologically, first, we opted for a window size of uneven pixels to have a clear central pixel to which assign the standard

deviation values. Second, we wanted to ensure for our calculations of land surface temperatures that our windows included at least 3 × 3 pixels of the original Landsat TIRS data, which has an original resolution of 100 m, prior to the downscaling by the USGS (Elsen et al., 2020) to ensure robust calculations even if some pixels were missing due to clouds contamination. Third, a window size of 11 × 11 pixels is a medium size in the range of 3x3 to 101 × 101 pixels for which first-order texture measures are highly correlated (Culbert et al., 2012; St-Louis et al., 2006), which is why we assumed that it was not necessary to conduct our analyses for multiple window sizes.

2.5. Spatio-temporal patterns of vegetation greenness and land surface temperature

To obtain the spatio-temporal patterns of vegetation greenness and land surface temperature, we integrated the inter-annual and spatial variability indices. First, we classified the pixels of each index (CV_EVI_SOS, CV_LST_SOS, standard deviation texture of EVI and standard deviation texture of LST) into high and low values based on the quantile method. Second, we integrated the following maps: (a) inter-annual variability in the phenology of vegetation greenness (250-m resolution) versus spatial variability of vegetation greenness (30-m resolution summarized in 330-m windows), and (b) inter-annual variability in the seasonality of land surface temperature (1-km resolution) versus spatial variability of land surface temperature (30-m resolution summarized in 330-m windows). Prior to integration, we resampled the input datasets with nearest neighbor resampling to match the resolution of our coarsest dataset. We thus produced two maps of spatio-temporal variability, one for vegetation greenness at 250-m resolution, and one for land surface temperature at 1-km resolution (See Fig. 2, step 3).

2.6. Hotspots of biodiversity conservation concern

Our second objective was to identify where both phenological and seasonal variability was of high, low, or medium conservation concern (Table 1). We based these analyses on the upper and lower quantiles in our maps of the spatio-temporal variability of vegetation greenness and land surface temperatures. We mapped hotspots by identifying clusters of pixels in either the high and low conservation concern category, using the Getis-Ord Gi* statistic (Getis and Ord, 1992) as follows:

$$G_i^* = \frac{\sum_{j=1}^{n} w_{i,j}x_j - \overline{X}\sum_{j=1}^{n} w_{i,j}}{S\sqrt{\frac{n\sum_{j=1}^{n} w_{i,j}^2 - \left(\sum_{j=1}^{n} w_{i,j}\right)^2}{}}}; \overline{X} = \frac{\sum_{j=1}^{n} x_j}{n}; S = \sqrt{\frac{\sum_{j=1}^{n} x_j}{n} - \overline{X}^2} \quad (1)$$

where x_j is the attribute value for feature j, $w_{i,j}$ is the spatial weight between feature i and j, and n is the total number of features. The Gi* statistic returns for each feature in the dataset a z-score. Large positive z-scores values (>2.58, confidence value of 99%) indicate hotspots.

To perform the hotspot analysis, we based the analyses only on forests, shrublands and grasslands, avoiding capturing variability in crops and fragmented areas that could increase heterogeneity and could be negatively related with biodiversity. To do so, we masked the maps of spatio-temporal variability based on a landcover map of Argentina (INTA, 2009) and we removed all croplands, bare soil, roads, and urbans areas from further analyses.

We also identified hotspots of high and low conservation concern based on the variability of both greenness and land surface temperature together. To do so, we mapped the areas where both the greenness and the temperature hotspot maps indicated either high conservation concern or low conservation concern, and calculate for each ecoregion and province the percentage of the areas in either category.

3. Results

3.1. Inter-annual variability in the phenology of vegetation greenness and in the seasonality of land surface temperature

We assessed the inter-annual variability in the phenology of vegetation greenness based on three indices (Table 2; Fig. S2). These three indices were moderately correlated, with Pearson's correlation indices ranging from 0.56 to 0.66 (Fig. S3). Our principal component analysis of the three phenological metrics showed that most of the variance in the first principal component (Eigenvalues = 77.4%) was related to CV_EVI_SOS (r = 0.78; Table S1), which is why we selected this index for further analyses of the inter-annual variability of the phenology in vegetation greenness.

The coefficient of variation of the start of the growing season exhibited a wide range of values across Argentina, reaching > 40% in some areas (Fig. S2a). In particular, CV_EVI_SOS was low (mean CV < 15%) in the Patagonian forests, Dry Chaco, Alto Parana Atlantic forests, and Southern Andean Yungas ecoregions, and also in Tucumán and Misiones provinces, which are dominated by native forests. However, CV_EVI_SOS was high (mean CV >25%) in the Pampa, Parana flooded savanna, Espinal, southern Patagonian steppe, northern High Andes and southern Puna ecoregions, and in Entre Rios, Buenos Aires, Santa Fe, Santa Cruz, La Pampa and Cordoba provinces, all of which are characterized by shrublands and grasslands (Fig. S4-1a,b). In contrast to strong inter-annual variability for the start of the growing season, we found little inter-annual variability at the end of the season and values of CV_EVI_EOS (Fig. S2b) were low across the country (maximum CV of 12%). The inter-annual variation in the length of the growing season (CV_EVI_LOS, Fig. S2c) was also generally low, and the highest values occurred in the Pampa and Espinal, and in small, dispersed areas of the Dry Chaco ecoregions.

Similarly, we assessed inter-annual variability in the seasonality of land surface temperature based on three indices (Table 2; Fig. S5). The three land surface temperature indices were more strongly correlated than those for vegetation greenness, with Pearson's correlation indices ranging from 0.69 to 0.90 (Fig. S3). In the PCA, the first component PC1 explained 95.2% of the variability and was highly correlated with the index CV_LST_SOS (r = 0.93; Table S2), which is why we chose it as our index of inter-annual variability in the seasonality of land surface temperature.

The Alto Parana Atlantic forests, Dry Chaco, and Humid Chaco ecoregions in the north of the country had the highest inter-annual variations in temperature at the start and end of the growing season (CV_LST_SOS and CV_LST_EOS), and between the two, CV_LST_SOS was substantially higher (up to 20-40%) than CV_LST_EOS (<20%; Fig. S5a, b). The Alto Parana Atlantic forests, Southern Andean Yungas, and Humid Chaco ecoregions had the highest variability in CV_LST_SOS (mean >22%), as had Chaco, Formosa and Misiones provinces, while the High Monte, Patagonian steppe, and Low Monte regions had lowest variability, as well as Rio Negro, Chubut and Neuquén provinces (Fig. S4-2a,b). The length of the growing season (CV_LST_LOS) did not vary markedly across the country (max <10%; Fig. S5c).

Comparing the inter-annual variability in the phenology of vegetation greenness with the seasonality of land surface temperature, we were surprised to find that their correlation was generally weak, and often negative, i.e., that the areas where inter-annual variability in greenness was high were not the same areas where inter-annual variability in temperature was high. Specifically, CV_EVI_SOS and CV_LST_SOS were weakly negatively correlated across Argentina (r = -0.19; Fig. 3a, b), but the relationship varied within our different ecoregions (Fig. 3c) and provinces. For example, in the Southern Andean Yungas (Fig. 3-1a,b) and Humid Chaco (Fig. 3-2a,b), the correlation was moderately negative (r = -0.38 and r = -0.22, respectively). Among the provinces, Rio Negro and Salta provinces had the highest negative correlation (r = -0.30). In contrast, within the High Andes (Fig. 3-3a, b) and Mesopotamian

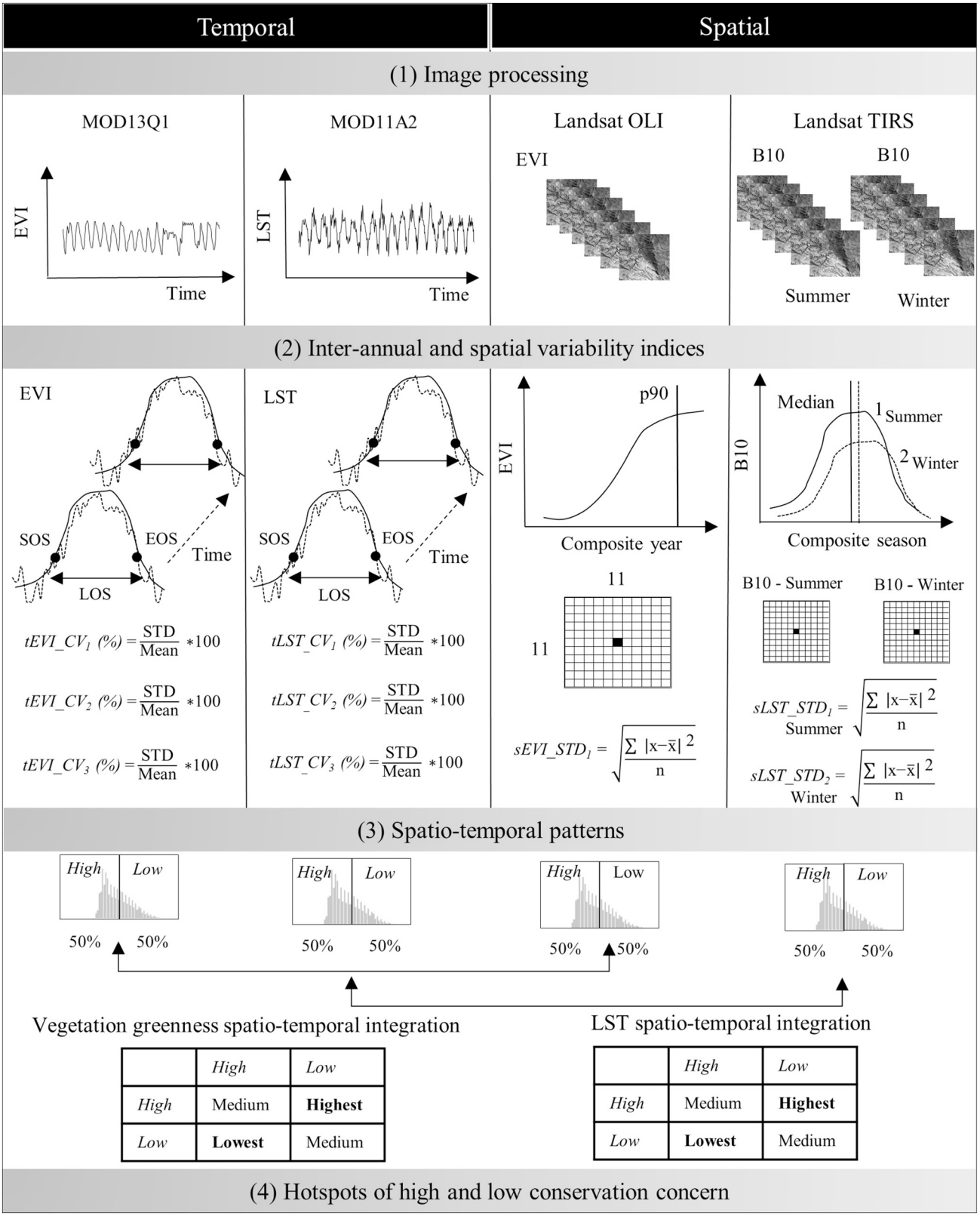

	High	*Low*
High	Medium	**Highest**
Low	**Lowest**	Medium

	High	*Low*
High	Medium	**Highest**
Low	**Lowest**	Medium

Fig. 2. Flowchart of the steps that we took to calculate our indices and identify potential areas of biodiversity conservation concern: (1) image processing of MOD13Q1 (MODIS 16-day Vegetation Indices), MOD11A2 (MODIS 8-day Land Surface Temperature), Landsat OLI (Operational Land Imager), and Landsat TIRS (Thermal Infrared Sensor); (2) inter-annual variability indices (t) based on the coefficient of variation (CV) of phenological and seasonality metrics from EVI (Enhanced Vegetation Indices) and LST (Land Surface Temperature), including the start (SOS), the end (EOS), and the length of the growing season (LOS); and spatial variability indices (s) based on the standard deviation (STD) of EVI and B10-LST; (3) integrating inter-annual and spatial variability to identify areas of high, medium, and low conservation concern due to inter-annual variability in phenology and temperature seasonality.

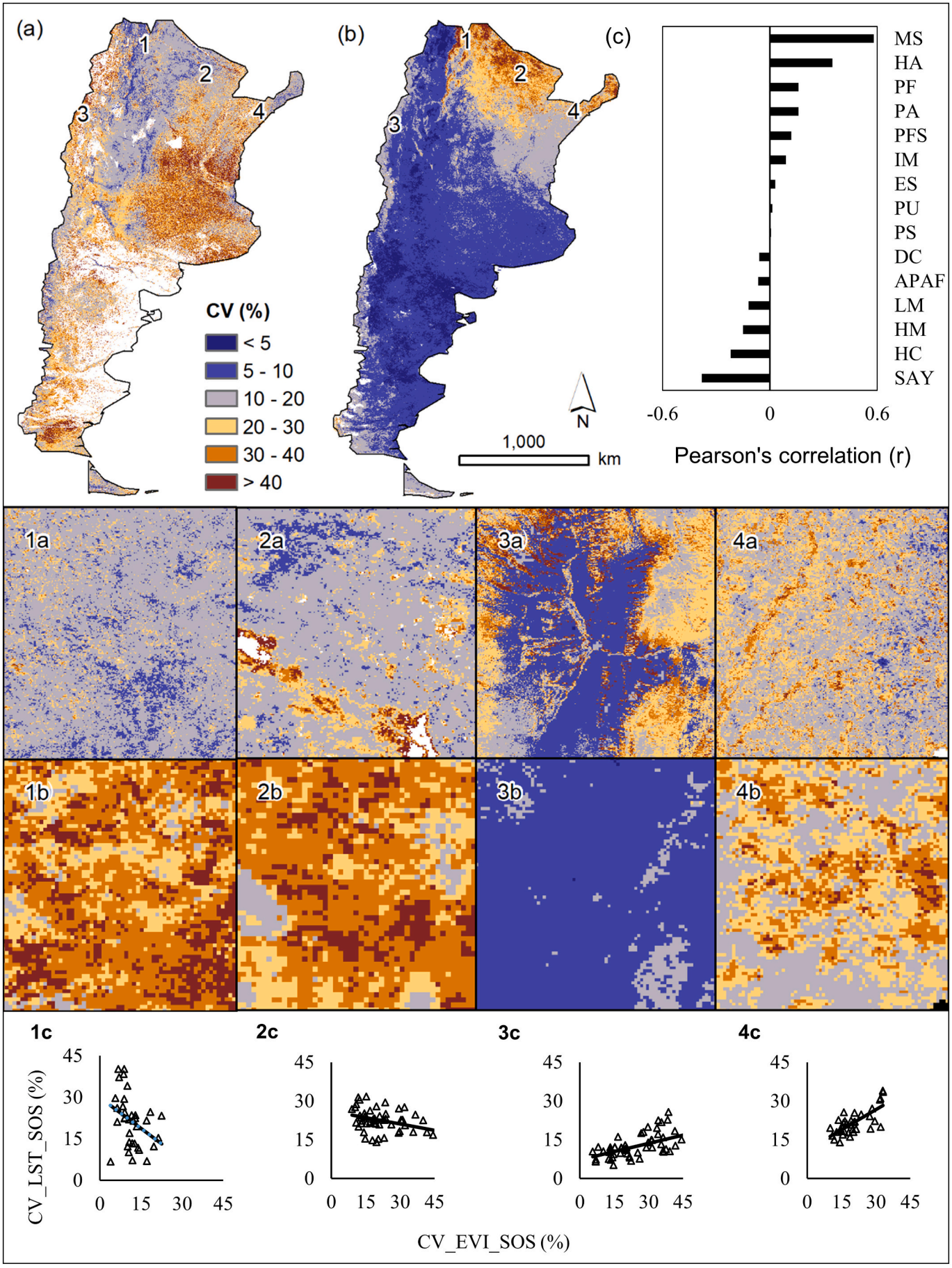

(caption on next page)

Fig. 3. Inter-annual variability of the start of the season according to (a) vegetation greenness (CV_EVI_SOS) and (b) land surface temperature (CV_LST_SOS), and (c) Pearson's correlation (r) between these two indices within ecoregions. Numbers (1-4) show detailed patterns within the Southern Andean Yungas (SAY), Humid Chaco (HC), High Andes (HA), and Mesopotamian savanna (MS) ecoregions, respectively (patterns for vegetation greenness in the top row, patterns for land surface temperature in the bottom row). White areas in maps reflect those with <15 observations of seasonal metrics. Insets 1abc and 2abc show regions and scatterplots where the correlation between two indices is negative, while insets 3abc and 4abc show regions where it is positive.

savanna ecoregions (Fig. 3-4a, b), CV_EVI_SOS and CV_LST_SOS were moderately positively correlated ($r = 0.25$ and $r = 0.58$, respectively). At province level, San Ruan had the maximum positive correlation ($r = 0.23$).

3.2. Spatial variability in vegetation greenness and land surface temperature

We assessed spatial variability of vegetation greenness by calculating the standard deviation of Landsat 8 EVI values in an 11 × 11 pixel moving window. The highest spatial variability in vegetation greenness across Argentina occurred in ecoregions covered by forests (i.e., the Southern Andean Yungas, Alto Parana Atlantic forests, Patagonian forests, Dry Chaco, Humid Chaco, and Parana flooded savanna) and croplands (Pampa; Fig. 4a,b). We wondered if the high spatial variability in forests might be due to a higher mean EVI there. In general, it is likely that spatial variability in EVI differs among land cover types, due to differences in the range of reflectance values of dominant plants (e.g., trees vs. grasses). However, among the natural land cover classes, forests, grasslands and wetlands had very similar means and ranges of standard deviations (Fig. S6), and while the mean for shrubland was lower, there was still a considerable range of standard deviations within that class, suggesting that the EVI data was sensitive enough to capture spatial variability in all land cover classes across Argentina. Forests and grasslands had very similar means and ranges of variability and even though the mean of the standard deviation was lower for shrublands, there was still a considerable range of standard deviations within that class. The only class that had a clearly higher mean of standard deviations was cropland, which may be due to more fragmented land cover where croplands are common. In addition, we calculated the correlations between mean and standard deviation of EVI for each land cover type, and found only weak to moderate correlations, ranging from $r = 0.12$ to $r = 0.55$ (Fig. S7).

Spatial variability in vegetation greenness, both within and between land cover classes, varied considerably within our ecoregions. For example, in the Alto Parana Atlantic forests, we found high spatial variability in vegetation greenness in drainage areas (Fig. 4-1a,b,c). In the Southern Andean Yungas ecoregion, we found high spatial variability in greenness in areas dominated by closed forests (Fig. 4-2a,b,c). As we expected, in areas dominated by croplands (Pampa), spatial variability in vegetation greenness was high where crops and tilled ground with no cover were in close proximity (Fig. 4-3a,b,c). Within Patagonian forests (Fig. 4-4a,c,d), the index captured variability in homogeneous land cover classes, highlighting texture's ability to characterize fine scale variability. Among the ecoregions, Patagonian forest, Parana flooded savanna and Pampa had the highest spatial variability of vegetation greenness (standard deviation > 0.06), while Puna, Low Monte and High Andes had the lowest values (standard deviation < 0.01, Fig. S8a). Among the provinces, Terra Del Fuego and Buenos Aires had the highest spatial variability, while Rio Negro, Santa Cruz and Catamarca had the lowest spatial variability in vegetation greenness (Fig. S8b).

Land surface temperatures during summer and winter were moderately positive correlated ($r = 0.46$). During summer, the highest LST values were concentrated in northwestern Argentina while during winter, LST increased from south to north (Fig. 5a, b). High Andean and Puna ecoregions, and San Ruan and Catamarca provinces, had the highest LST values in both summer and winter (Fig. S8c-f). The spatial variability in land surface temperature (i.e., the standard deviation of LST in a moving window of 11 × 11 pixels) during summer and winter was also moderately positively correlated ($r = 0.60$) (Fig. 5c, d), highlighting the importance of using the variability in both summer and winter together to guarantee that the extremes variability in both seasons are considered. When we combined the spatial variability of land surface temperature in both summer and winter, we found that it was highest in areas of strong topographic relief (e.g., in the Andes Mountains and Puna ecoregions), and lowest in parts of the Dry Chaco, Low Monte, Humid Chaco, Espinal and Patagonian steppe ecoregions (Fig. 5e).

Finally, the spatial variability of vegetation greenness and of land surface temperature were weakly correlated across Argentina ($r = 0.22$ based on summer temperature, and $r = 0.02$ based on winter). Within ecoregions, maximum values occurred during summer in the Pampa ($r = 0.40$), Patagonian steppe ($r = 0.37$), Espinal ($r = 0.35$), and Low Monte ($r = 0.34$; Table S3). Within provinces, spatial variability of vegetation greenness and summer land surface temperature spatial variability were highly correlated in Rio Negro ($r = 0.52$), Chubut ($r = 0.51$), Neuquén ($r = 0.51$) and Santa Cruz ($r = 0.50$) (Table S4).

3.3. Areas of potential conservation concern due to phenological and seasonal variability

We combined our maps of inter-annual variability in the phenology of vegetation greenness and in the seasonality of land surface temperature (Fig 6a) with their respective maps of spatial variability (Fig 6b), to identify potential areas of high, medium, and low conservation concern due to phenological and seasonal variability (Table 1, Fig. 6c).

The hotspots of high and low conservation concern that we mapped based on vegetation greenness (Fig. 6, 1d) differed considerably from those mapped based on land surface temperature (Fig. 6, 2d). Based on the vegetation greenness, hotspots of conservation concern were concentrated in the High Andes, Puna, Ibera marshes, south of High Monte, north of Low Monte, west part of Patagonian steppe and in parts of Espinal ecoregion. At province level, hotspots of conservation concern based on the spatio-temporal patterns of vegetation greenness were in Salta, Catamarca, La Rioja, San Ruan, Mendoza, San Luis, La Pampa, Chaco, Santa Fé, Entre Rios, Corrientes, Rio Negro, Chubut and Santa Cruz. Areas of low conservation concern were concentrated in the Alto Parana Atlantic forests, Southern Andean Yungas, Patagonian forest, north of Puna, some parts of Chaco, Mesopotamian savanna, and Pampa ecoregions, and in the following provinces: Misiones, Tierra del Fuego, and some parts of Salta, Buenos Aires, Chubut, Rio Negro, Neuquén, Córdoba, San Luis, Jujuy, Chaco, and Catamarca. Hotspots of conservation concern based on the spatio-temporal patterns of land surface temperature were quite different. For example, the Alto Parana Atlantic forests in northeastern Argentina were of low conservation concern based on vegetation greenness, but of high conservation concern based on land surface temperature.

In a final step, we identified hotspots of high and low conservation concern based on the spatial agreement between vegetation greenness and land surface temperature derived maps of conservation concern (Fig. 7). The high-conservation concern areas were in the northern region predominantly within the Humid Chaco (62,586 km^2), Espinal (51,930 km^2) and Ibera Marshes (33,331 km^2) ecoregions and in the south in a small portion of the Patagonian steppe in Santa Cruz province (21,024 km^2). Humid Chaco, Ibera Marshes, Mesopotamian savanna and Parana flooded savanna ecoregions have more than 50% of their area within the hotspot of high-conservation concern (Fig. 7a). In Humid

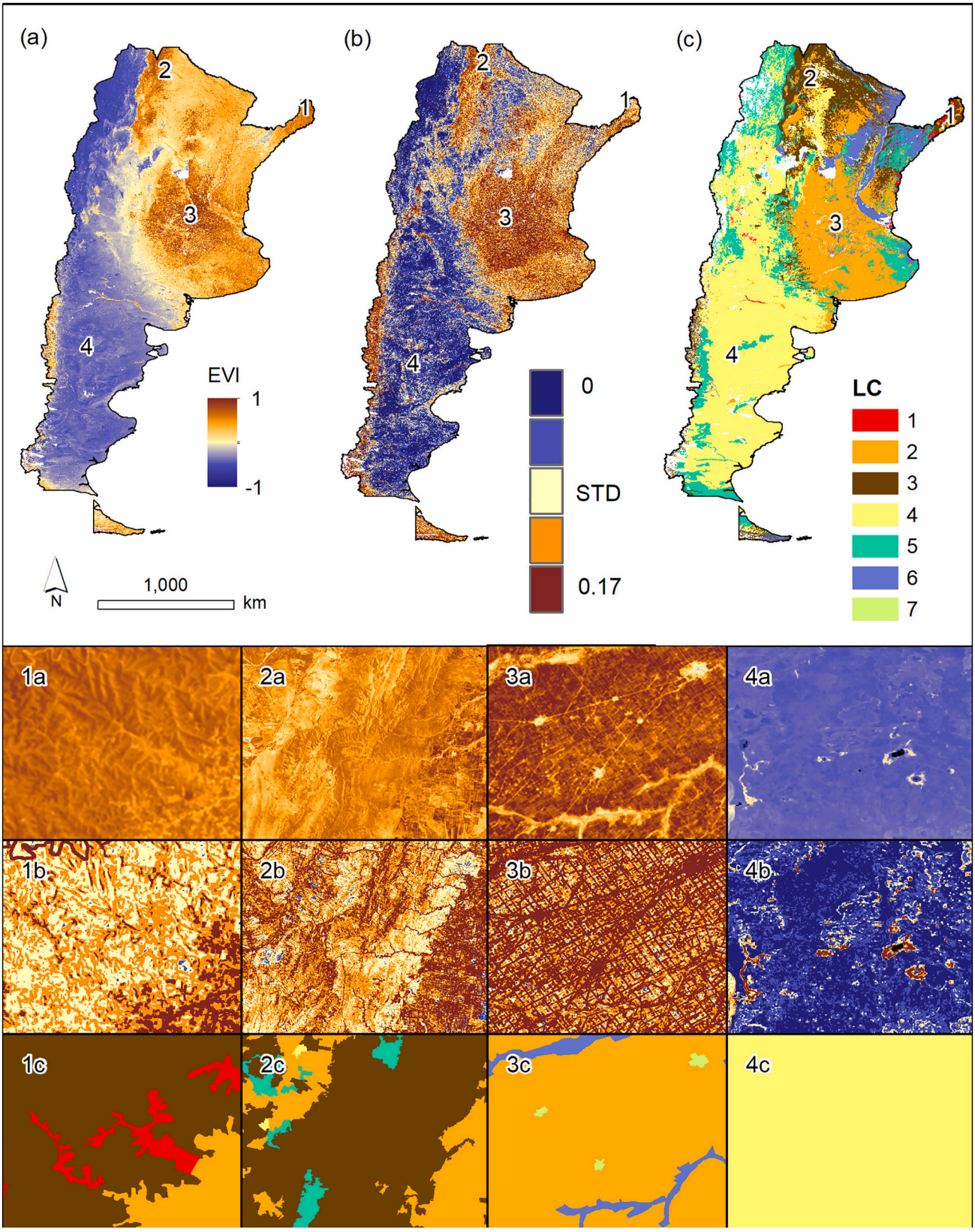

Fig. 4. (a) Enhanced vegetation index (EVI) derived from Landsat 8 Surface Reflectance Tier 1 composite from 2013 to 2018, (b) vegetation spatial variability, defined as the standard deviation (STD) of EVI captured in a moving window of 11 × 11 pixels, (c) landcover map, with the following classes: (1) forest plantations, (2) crops, (3) native forests, (4) shrublands, (5) grasslands, (6) herbaceous wetlands, and (7) urban areas (source: https://inta.gob.ar/sites/default/files/script-tmp-informe_tecnico_lccs.pdf; INTA, 2007), Numbers (1-4) depict detail of EVI (top row), vegetation spatial variability (middle row), and land cover (bottom row) and column numbers indicate locations of insets on country scale maps.

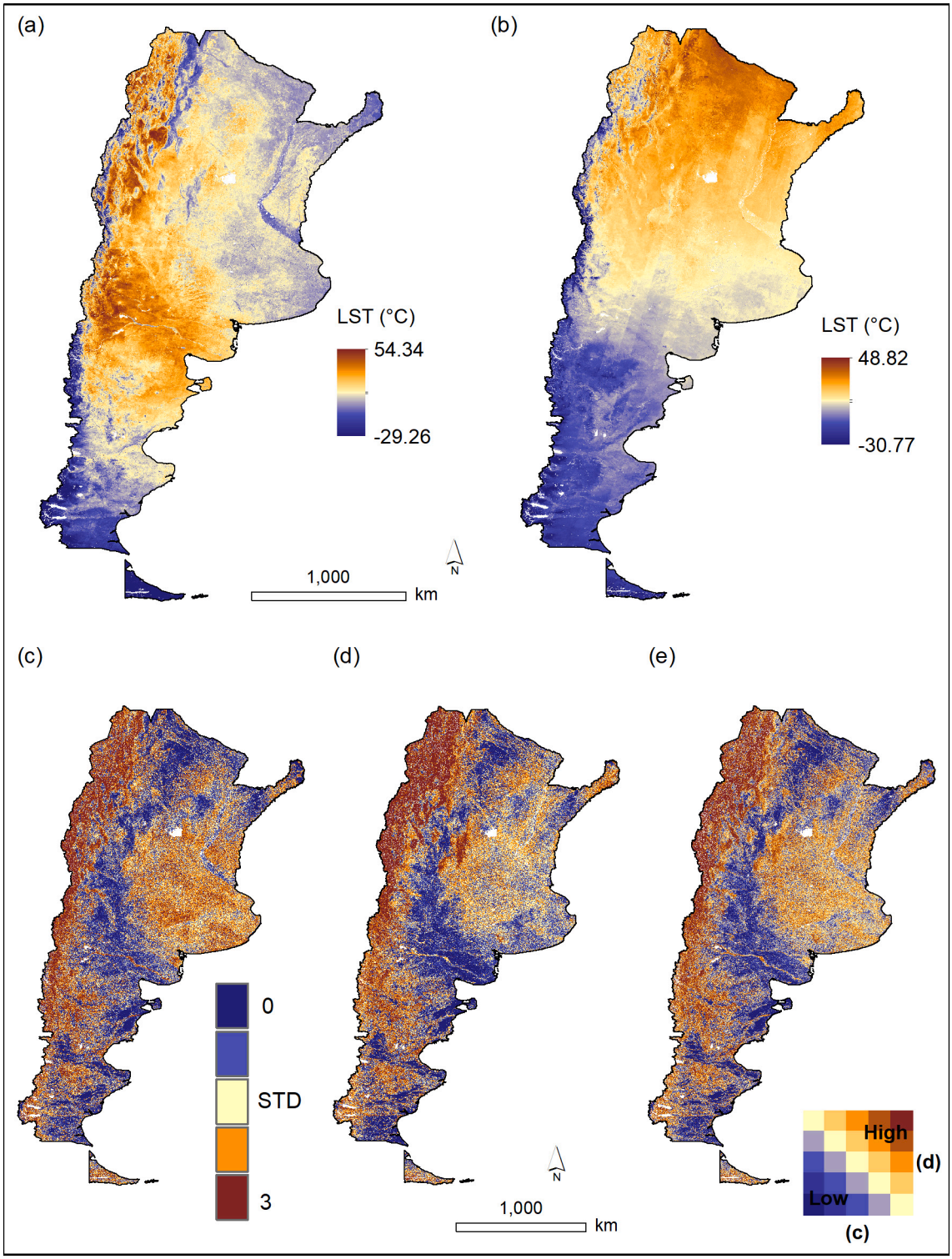

Fig. 5. (a) Land surface temperature (LST) based on B10 (brightness temperature) from Landsat 8 TIR data for summer, (b) LST based on B10 (brightness temperature) from Landsat 8 TIR data for winter, (c) spatial variability in land surface temperature, defined as the standard deviation (STD) of LST captured in a moving window of 11 × 11 pixels, for summer, (d) winter, and (e) the interaction of spatial variability in land surface temperature for summer and winter.

Chaco, the hotspots of high conservation concern are mainly in Santa Fé and Chaco provinces, while in Ibera Marshes and Espinal ecoregions, hotspots of high conservation concern are mainly in Corrientes and Entre Rios provinces (Table S5). Among provinces, the high-conservation concern hotspots encompassed more than 50% of Corrientes and Santa Fe provinces and 45% of Entre Rios territory (Fig 7b). The high-conservation concern hotspots are mainly occupied by wetlands (45%), followed by grasslands (26%), forests (22%) and shrublands (7%).

Low-conservation concern hotspots are in the northwest (106,272 km^2) and central-west of Argentina (63,643 km^2), mainly in Puna within Jujuy (21,232 km^2) and Salta (14,656 km^2) provinces and Patagonian steppe within Neuquén, Rio Negro and Chubut provinces (Fig 7; Table S6). Southern Andean Yungas and Patagonian forests have more

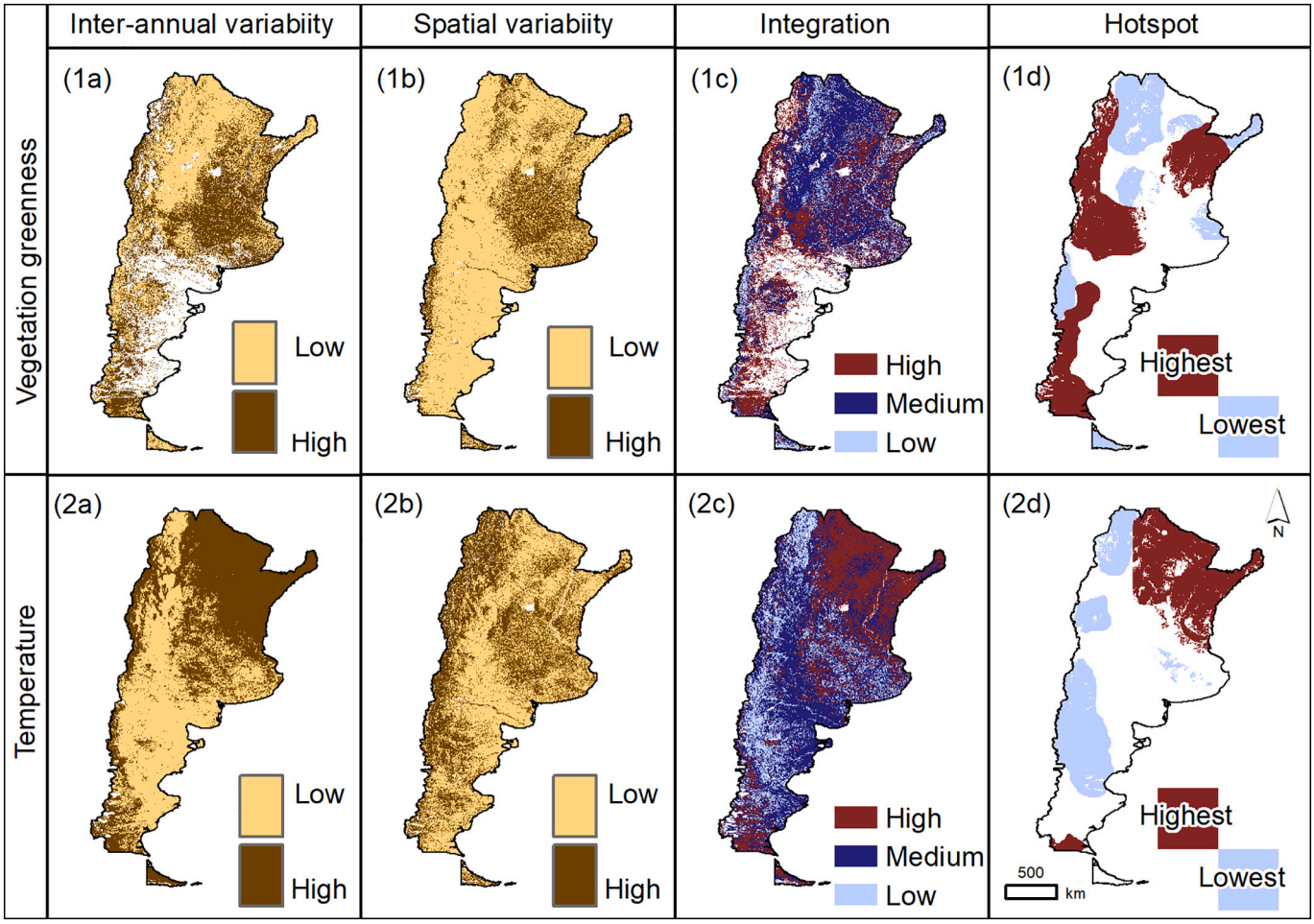

Fig. 6. Areas of high and low conservation concern based on (1) vegetation greenness and (2) land surface temperature: (a) inter-annual variability in phenology, (b) spatial variability, (c) integration between inter-annual and spatial variability, and (d) hotspots maps according to the Getis-Ord Gi* statistic. White areas in (a) and (c) had <15 phenology metrics observations.

than 50% of their areas inside the hotspot of low-conservation concern (Fig. 7a). Among the provinces, low-conservation concern areas cover 90% of Jujuy, 50% of Neuquén, 30% of Tucuman, 20% of Catamarca and Rio Negros and 10 % of Chubut provinces. The main land cover classes within low-conservation concern hotspots are shrublands (43%), grasslands (32%) and forests (25%).

4. Discussion

4.1. Inter-annual and spatial variability indices

High inter-annual variability in the phenology of vegetation greenness and in the seasonality of temperature presents a threat to the survival of many species, but high spatial variability enhances resilience to this threat. We generated indices to capture the inter-annual variability and spatial variability of vegetation greenness and land surface temperature so that we could identify hotspots of high and low conservation concern for biodiversity conservation. We found strong differences among the ecoregions and the provinces of Argentina in terms of the magnitude of both inter-annual and spatial variability, suggesting that species in different areas face very different threats from variability in phenology and temperature seasonality. Spatio-temporal variability in vegetation greenness was only weakly correlated with land surface temperature. That suggests that it is valuable to map both when assessing the threats from phenological and seasonal variations. By combining our maps of inter-annual and spatial variability, we identified the areas of highest conservation concern due to phenological and seasonal variability (i.e., those areas where high inter-annual variability posed a strong threat, and where low spatial variability meant that resilience is low), as well as those of low conservation concern where the threat is low and resilience is high.

The time series of MODIS EVI and LST data provided a powerful dataset to calculate inter-annual variability for the phenological and seasonal metrics (start, end and length of the growing season). Most phenological metrics are derived from time series of vegetation indices, such as EVI and NDVI (Zeng et al., 2020). However, vegetation indices sometimes are not able to detect phenological patterns due to low intra-annual variation in greenness, especially where vegetation is very sparse (Liu et al., 2016) (see blank areas in Fig. 3a). In areas where the phenology of vegetation and seasonality of temperature have similar patterns, land surface temperature changes over the course of a year can play a complementary role when assessing phenology, especially in areas, such as evergreen forests, where estimates of the start and end of the season tend to be more variable due to limited phenological variability in canopy greenness (Liu et al., 2016).

Climate change can result in changes in either temperature or in the seasonality of temperature. Changes in temperature, also referred to as temperature magnitude, cause a change in the statistical distribution of temperature (e.g., an increased mean), while temperature temporal position describes the change in timing (i.e., date) of a specific event (Waldock et al., 2018). Temperature temporal position can change over time while the statistical distributions remains the same (Garcia et al.,

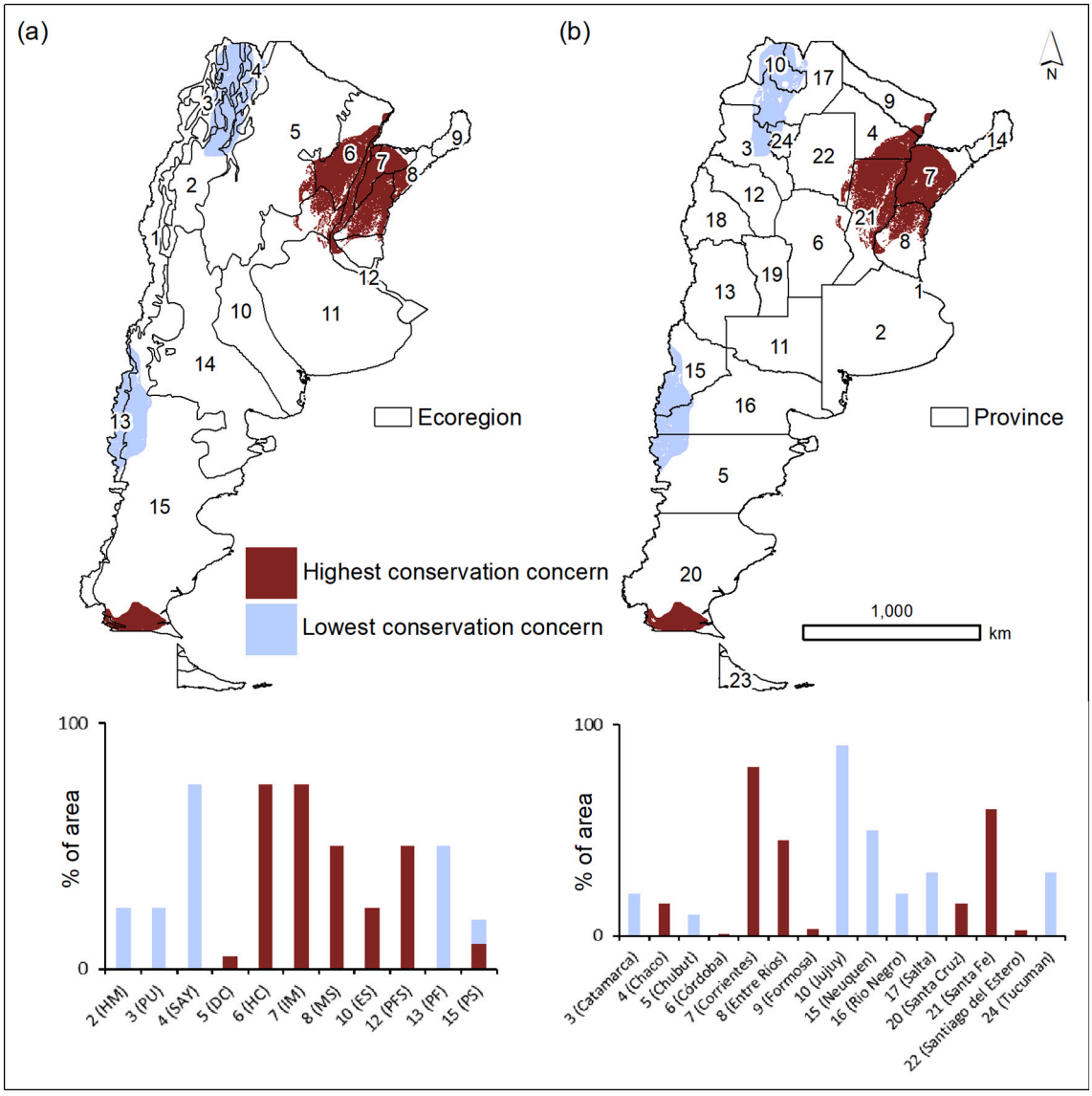

Fig. 7. Hotspots of highest and lowest conservation concern by (a) ecoregion and (b) province. Abbreviations of ecoregions: 1 - High Andes (HA), 2 - High Monte (HM), 3 - Puna (PU), 4 - Southern Andean Yungas (SAY), 5 - Dry Chaco (DC), 6 - Humid Chaco (HC), 7 - Ibera marshes (IM), 8 - Mesopotamian savanna (MS), 9 - Alto Parana Atlantic forests (APAF), 10 - Espinal (ES), 11 - Pampa (PA), 12 - Parana flooded savanna (PFS), 13 - Patagonian forests (PF), 14 - Low Monte (LM), 15 - Patagonian steppe (PS). Provinces: 1 – Autonomous city of Buenos Aires, 2 – Buenos Aires, 3 – Catamarca, 4 – Chaco, 5 – Chubut, 6 – Córdoba, 7 – Corrientes, 8 – Entre Rios, 9 – Formosa, 10 – Jujuy, 11 – La Pampa, 12 – La Roja, 13 – Mendoza, 14 – Misiones, 15 – Neuquén, 16 – Rio Negro, 17 – Salta, 18 – San Juan, 19 – San Luis, 20 – Santa Cruz, 21 – Santa Fé, 22 – Santiago del Estero, 23 – Tierra del Fuego, 24 – Tucumán.

2014; Loarie et al., 2009). For example, changes in date of specific events, e.g., an earlier start and end of the season, is a change in temporal position but not a change in statistical distribution. Thus, research that focuses strictly on directional change of means and not on changes in the seasonality, may underestimate the effects of climate change on biodiversity patterns and responses (Waldock et al., 2018). This is why we calculated the inter-annual variability in the seasonal dates of temperature variability (i.e. CV_LST_SOS) to capture seasonal variability. Having said that, we did not include an analysis of the trends, because the MODIS record of twenty years is fairly short. Hence, we acknowledge that describing seasonal variations alone does not capture the full effect of climate change. However, we opted to focus on seasonal variation because that allowed identification of areas of high and low conservation concern assuming that climate change will result in higher climatic variability and more frequent extreme events.

We found considerable differences in the patterns of inter-annual variability in the phenology of vegetation greenness and in the seasonality of land surface temperature across Argentina. The correlation between CV_EVI_SOS and CV_LST_SOS was surprisingly weak across the entire country (r = -0.19), and also fairly weak in most ecoregions and provinces. However, in some ecoregions we found moderately positive (r = 0.58) to negative (r = -0.38) correlations. Our analyses were not designed to identify the reasons why the differences in the inter-annual variability patterns of greenness and land surface temperature were weak to moderate in Argentina. However, ecoregions in Argentina are diverse in terms of vegetation and topography. Some reasons for the weak and moderate relationships could be that in general, vegetation growth acclimates to rapid temperature warming and becomes less affected by climate change (Hikosaka et al., 2006), or due to topographic effects. Other reasons could be the lagged response of greenness to water limitation (An et al., 2018), and relationships affected by vegetation type (Liu et al., 2018; Wang et al., 2008).

Our results combined with those from prior studies thus suggest that examining the inter-annual variability in the phenology of vegetation

greenness and in the seasonality of land surface temperature is both necessary and valuable because one is not a good proxy for the other, and some species will respond more strongly to greenness (e.g., herbivores), and others to temperature (e.g., exotherms). Although the patterns in inter-annual variability in the phenology of vegetation greenness and in the seasonality of land surface temperature were not highly spatially correlated, there was strong inter-annual variability in the start of the growing season (greenness) and spring warm-up (temperature) from 2001 to 2018. Climate change may have caused this variability either via a trend over time, so that all later years are considerably higher than all early years, or by increasing year-to-year differences and the frequency of extreme year. Our analyses were not designed to distinguish between these potential causes for higher inter-annual variability, but this variability is concerning for species either way. Indeed, high variability of spring onset may cause phenological mismatches between animals and plants (Thackeray et al., 2010), especially if the amount of variability that we found is greater than in decades prior to our study period (Allstadt et al., 2015; Schweiger et al., 2008).

Image texture based on the standard deviation of EVI and LST from Landsat 8 data captured vegetation greenness and land surface temperature spatial variability, and thus helped to identify areas where there are enhanced resilience to the threat of high inter-annual phenological and seasonal variability. We found the highest spatial variability in land surface temperature in areas of high topography relief and highest spatial variability of vegetation greenness in areas cover by forests. High spatial variability can result from different processes, including high geodiversity. Geodiversity, defined as 'the diversity of geological (rocks, minerals, fossil), geomorphological (land form, processes) and soil features" (Gray, 2008) is a strong driver of biodiversity patterns worldwide (Gill et al., 2015). Environmental conditions can enforce physiological limitations, while diversity of topographic, habitat and geophysical features can lead to niche diversification (Zarnetske et al., 2019). For example, geodiversity components (landforms, hydrology and surface materials), climate, topography and land cover variability improved understanding of the relationship between species richness and abiotic heterogeneity at multiple spatial scales (Bailey et al., 2017) and have been suggested as key variables for identifying refugia (Keppel et al., 2015).

The spatial variability of vegetation has a strong influence on biodiversity patterns (Stein et al., 2014), and high variability promotes species diversity by increasing the number of available niches (Tews et al., 2004), promotes speciation via genetic isolation in species with low mobility (Thorpe et al., 2008) and increases the availability of microhabitats that provide refugia from adverse conditions and climatic extremes (Keppel et al., 2012). This increased access to a variety of microhabitats, in particular, links vegetation spatial variability to increased resilience against climate change, both in the context of short-term (Piha et al., 2007) and long-term changes (Virah-sawmy et al., 2009). Spatial variability in the vegetation greenness also increases environmental resilience in the face of changes in climate by providing a buffer against the loss of ecosystem processes (Turner et al., 2013) and promoting functional redundancy (Feit et al., 2019). Indices of vegetation greenness characterize net primary productivity (Sims et al., 2006), and regions with higher overall productivity can support more species (Currie, 2020). Texture measures derived from vegetation indices provide information about the spatial patterning of productivity that make them strong predictors of bird richness patterns (Farwell et al., 2020; St-Louis et al., 2009).

The spatial variability of land surface temperature drives species richness patterns in similar ways as that of vegetation greenness. For example, spatial variability in temperature can increase species richness through the creation of thermal niches that can be exploited by organisms adapted to unique thermal environments (Letten et al., 2013). Furthermore, species can utilize environments with high spatial variability to find refugia during times of temperature extremes, thereby minimizing their exposure to hot and cold temperatures (Scheffers et al., 2014). Areas of high spatial variability in temperature are also particularly important for climate-sensitive species, including species with poorer thermoregulatory capacity and narrow thermal tolerances (Elsen et al., 2020). Taken together, regions with high spatial variability of temperature provide resilience to possible threats due to high inter-annual variability in temperature. Our recommendations are scale-dependent though, and the relationship between temperature and biodiversity will likely differ at different scales (Bailey et al., 2017; Zarnetske et al., 2019). Having said that, at the scales that we measured, while temperature changed markedly in Argentina (Fig. 5a, b), the regions with high spatial variability were generally the same in summer and winter (Fig. 5c–e).

We analyzed inter-annual and spatial variability indices at the scale of the country of Argentina and at finer scales (ecoregions, provinces, and their intersection). We did not perform a grain size scale analysis because our inter-annual variability indices are limited to 1-km and 250-m resolution. Similarly, in our analysis of spatial variability we also did not test grain size scales by changing the moving window size (30-m resolution summarized in 330-m windows) because first-order texture measures, such as standard deviation, are highly correlated from 3x3 to 101 × 101 pixels (Culbert et al., 2012; St-Louis et al., 2006). However, phenological and seasonal metrics, and image textures calculated from higher spatial resolution images may provide better characterization of the spatio-temporal patterns of vegetation greenness and land surface temperature. To interpret our results in greater detail, we intersected boundaries of ecoregions and provinces to identify hotspots of high conservation and low conservation concern (Tables S5, S6). Because our analysis are in the same spatial grain, the only differences we found are in the result's interpretation.

4.2. Conservation and management implications

The hotspots of biodiversity conservation concern provide important information for conservation prioritization. For example, in areas where land use plans are mandated in Argentina, such as forests (Argentina National Forest Law N° 26,331), making strategic adjustments to existing land use zones can enhance biodiversity conservation (Martinuzzi et al., 2018). Argentina currently protects less than 9% of its terrestrial land area (UNEP-WCMC, 2020), which means it would need to almost double the size of its current protected area estate to meet international targets set by the Convention on Biological Diversity (17% of terrestrial and inland water areas). Our approach of integrating spatio-temporal indices of vegetation greenness and land surface temperature allowed us to identify regions where the conservation concerns due to phenological and seasonal variability are high or low.

Areas of low conservation concern are those where inter-annual variability is low, and spatial variability is high, which means that the likelihood of mismatches between species and resources is lower and resilience against high inter-annual variability is higher. Such regions are located in the forests of northwest and central-west Argentina, encompassing the Southern Andean Yungas, Patagonian forests, Puna, High Monte and a small part of the Patagonian steppe ecoregions (Fig. 7a) and provinces of Jujuy, Neuquén, Tucumán, Catamarca and Rio Negro (Fig. 7b). These areas have enhanced resilience to both phenological and seasonal variability and may be important areas for biodiversity conservation (Kerr and Packer, 1997). Adding protected areas in these regions may be effective ways of both protecting current patterns of biodiversity and maintaining the adaptive capacity to climate change (Lawler et al., 2015; Tingley et al., 2014). Argentina created most of the National Parks for purposes other than conservation of biodiversity. For example, some Parks were established at the border with other countries for geopolitical reasons, and many showcase unique landscapes with an emphasis on tourism (Vejsbjerg et al., 2014). Further, many of Argentina's natural ecosystems are not well represented by the protected area system (Martin and Chehébar, 2001; Rosas et al., 2017; Rosas et al.,

2019).

The hotspots of low conservation concern in northwest and central-west Argentina are classified as medium level of human influence (Lizárraga and Monguillot, 2020) and 26% of these areas are under protection (UNEP-WCMC and IUCN, 2020). In addition, 36%, 58% and 6% of the forests of northwest and central-west Argentina within our low-conservation concern hotspots areas are classified into Zones I (high conservation value forests), Zone II (medium conservation value forest) and Zone III (low conservation values forests), respectively, according to Argentina's National Forest Plan (Fig S9). Zone I includes forests critical for biodiversity and ecosystem services provisioning, in which only tourism, scientific research, and the gathering of non-timber products are allowed. However, Zone II allows productive activities such as grazing, silvopasture and sustainable harvesting of timber and non-timber products and Zone III include forests that can be converted to other land uses such as agriculture, pastures, or timber plantations. To improve biodiversity conservation in Argentina, forests classified as Zone II and III, that we classified as low conservation concern, should be included in Zone I given their high potential conservation value.

In contrast the areas of highest conservation concern are in the northeastern region, predominant in the Humid Chaco, Espinal, Ibera marshes, Mesopotamian savanna and Parana flooded savanna ecoregions (Fig. 7a) and in Corrientes, Santa Fé and Entre Rios provinces (Fig. 7b). These areas include large wetlands, along with forests, grasslands, lakes, and marshes (Neiff, 2001). These ecosystems host high species richness – more than 450 plants species, 50 fish species, 40 amphibian species, 50 reptile species, 350 bird species, and 70 mammal species (Ginzburg and Adámoli, 2006; Neiff, 2001). High inter-annual variability is likely to have negative effects for species dependent on the timing of key events linked to temperature and vegetation greenness as ecological cues (e.g., for reproduction or migration (e.g., for reproduction or migration). In addition, especially times of extreme temperatures in northeast Argentina may have a substantial negative impact on species if there are no thermal refugia, which is why high inter-annual variability integrated with low spatial variability is of high conservation concern. This is especially the case for species whose populations have already declined in association with land use change. For example, these areas in northeast Argentina harbor at least 22 globally threatened or near-threatened bird species that depend on grasslands, some in combination with adjacent wetlands (Azpiroz et al., 2012). Eliminating the existing pressures on wetlands (i.e., dam construction, land use change, drainage, etc.; Sica et al., 2018) and improving spatial variability by increasing the abundance and diversity of natural landcover in this highly modified region are promising approaches to mitigate the adverse effects of high phenological variability on biodiversity.

The northeastern region has been categorized as of conservation concern (Ferrer-Paris et al., 2019). Most of the vegetation types are highly degraded by human activities such as agriculture and cattle grazing, and these areas are classified under low, medium and high level of human influence, with protected areas around 10% (Lizárraga and Monguillot, 2020; UNEP-WCMC and IUCN, 2020). Key actions to promote higher spatial variability include increasing the protection of the remaining refugia habitats, restoring natural vegetation where possible, expanding protected areas with high spatial variability to maintain structural complexity, and connecting refugia with corridors to reduce barriers to movement (Braatz, 2012; Galatowitsch et al., 2009). For wetlands specifically, conservation actions should also include maintaining connectivity between the wetland and open water sources to improve water quality and food resources, restoring complex channel networks to provide habitat spatial variability, and improving landscape permeability and connectivity through native plant and stream restoration (Beller et al., 2019). All of these strategies bolster the resilience of habitats by helping species adapt to changing climate conditions.

We also identified regions of medium conservation concern where there is something of a balance between the threat of inter-annual variability and enhanced resilience from spatial variability, because both are either high or low (Fig. 6; see also Table 1). While the threat from high inter-annual variability may be offset by the higher resilience due to high spatial variability, and, similarly, low spatial variability may be offset by low inter-annual variability, it is not always clear which factor takes precedence for a given species. For example, species adapted to inter-annual variability are often also more resilient to habitat loss because they are better adapted to cope with the changing thermal environment resulting from physical changes to the landscape (Balmford, 1996; Srinivasan et al., 2019). Similarly, species adapted to low-land habitats characterized by low spatial variability in land surface temperatures may be highly threatened by changes in mean temperature, even if temperature seasonality patterns remain relatively stable over time (Colwell et al., 2008). Consequently, some regions that we categorized as having medium conservation concern may still warrant some conservation actions. However, regions characterized as having high inter-annual variability and low spatial variability likely are those that require the most urgent conservation attention.

4.3. Caveats and considerations

To develop our inter-annual variability indices, we focused on vegetation greenness and land surface temperature time series derived from MOD13Q1-Collection 6 (250-m resolution) and MOD11A2-Collection 6 (1-km resolution). We then derived phenology and seasonality metrics and computed their coefficient of variation among years. In doing so, we made the inherent assumption that the phenology of vegetation greenness is related to vegetation phenology, but we caution that the two are by no means identical. Numerous approaches based on MODIS products have been used to derive phenology metrics that are proxies of plant phenology at regional and global scales (Ganguly et al., 2010; Liu et al., 2016; Wu et al., 2014). However, while MODIS data clearly capture general phenological patterns of greenness across landscapes, species interactions sensitive to phenology occur at much finer spatial scales than are observable from MODIS and thus timing and magnitude should be viewed as approximations, and different from actual plant phenology (Zhang et al., 2017). Consequently, our results should be used to understand broad phenology patterns of vegetation greenness, and do not depict the fine- scale aspects of vegetation phenology (e.g., the timing of bud-burst, or flowering, in tree species with inconspicuous flowers), and other aspects of vegetation phenology for which the resolution for MODIS pixels is too coarse.

Furthermore, remote sensing derived phenology metrics should not be interpreted in the same way as field-based observations of vegetation phenology. Vegetation indices derived from remotely sensed images measure vegetation greenness at the pixel level and do not directly record specific phenological events (Atkinson et al., 2012), which is a common limitation of phenology studies based on remotely-sensed data (de Beurs and Henebry, 2005, 2010). For example, the phenology of vegetation greenness of evergreen forests is more challenging to measure than that of deciduous forests because absolute changes in greenness are smaller, which means there is likely some degree of bias in the seasonality metrics between forest types (Zeng et al., 2020). Some bias can also be introduced due to vegetation changes caused by diseases or plant stress (Vina et al., 2004) or by specific grazing and agricultural practices (Hall-Beyer, 2003; Wardlow et al., 2006). Lastly, the statistical methods to determine the start and end of the growing season also have limitations, and linking remotely sensed observations with field collected data is one of the major challenges inherent in remotely-sensed phenology studies (de Beurs and Henebry, 2004).

Despite these limitations though, satellite data are the only data source that can map phenology of greenness consistently for large areas, and our results establish a novel approach to assess the threat from phenological variability for larger regions. That makes them valuable for informing conservation and management action, in our case for Argentina.

5. Conclusion

Remotely sensed data provide a great opportunity to generate indices that capture the inter-annual and spatial variability of vegetation greenness and land surface temperature that can be analysed jointly to efficiently determine hotspots of high threat from, and with enhanced resilience to phenological and seasonal variability. Management actions can be targeted in order to reduce the threat, or strengthen the resilience of ecosystems in order to minimize biodiversity loss. The hotspots of high conservation concern that we mapped represent areas where increasing spatial variability in vegetation greenness and land surface temperature could have large conservation benefits, and where spatial variability is high already, we suggest that protection should strongly be considered in order to maintain the natural biodiversity heritage of Argentina. The remotely sensed indices we developed for Argentina are freely available at http://silvis.forest.wisc.edu/data/inter-annual-spatial-variability-indices.

Supplementary data to this article can be found online at https://doi.org/10.1016/j.rse.2021.112368.

Funding

We gratefully acknowledge support for this work by the National Aeronautics and Space Administration (NASA) Biodiversity and Ecological Forecasting Program, project 80NSSC19K0183. The associate editor and three anonymous reviewers made valuable comments that greatly strengthened our manuscript.

Author contributions

E.M.O.S was responsible for processing the remote sensing analysis and writing the paper. V.C.R and A.M.P were responsible for creating the research design, writing and editing. E.B. S.M, G.M.P, L.O.R, NP, L.N, L. S.F AND P.R.E were responsible for writing and editing. All authors discussed the results and contributed to the final manuscript

Declaration of Competing Interest

The authors declare that they have no known competing financial interests or personal relationships that could have appeared to influence the work reported in this paper.

References

2Albright, T.P., Pidgeon, A.M., Rittenhouse, C.D., Clayton, M.K., Flather, C.H., Culbert, P.D., Radeloff, V.C., 2011. Heat waves measured with MODIS land surface temperature data predict changes in avian community structure. Remote Sens. Environ. 115, 245–254. https://doi.org/10.1016/j.rse.2010.08.024.

Allstadt, A.J., Vavrus, S.J., Heglund, P.J., Pidgeon, A.M., Thogmartin, W.E., Radeloff, V. C., 2015. Spring plant phenology and false springs in the conterminous US during the 21st century. Environ. Res. Lett. 10 https://doi.org/10.1088/1748-9326/10/10/104008.

An, S., Zhu, X., Shen, M., Wang, Y., Cao, R., Chen, X., Yang, W., Chen, J., Tang, Y., 2018. Mismatch in elevational shifts between satellite observed vegetation greenness and temperature isolines during 2000–2016 on the Tibetan Plateau. Glob. Chang. Biol. 24, 5411–5425. https://doi.org/10.1111/gcb.14432.

Angeler, D.G., Allen, C.R., 2016. Quantifying resilience. J. Appl. Ecol. 53, 617–624. https://doi.org/10.1111/1365-2664.12649.

Atkinson, P.M., Jeganathan, C., Dash, J., Atzberger, C., 2012. Inter-comparison of four models for smoothing satellite sensor time-series data to estimate vegetation phenology. Remote Sens. Environ. 123, 400–417. https://doi.org/10.1016/j.rse.2012.04.001.

Azpiroz, A.B., Isacch, J.P., Dias, R.A., Di Giacomo, A.S., Fontana, C.S., Palarea, C.M., 2012. Ecology and conservation of grassland birds in southeastern South America: a review. J. Field Ornithol. 83, 217–246. https://doi.org/10.1111/j.1557-9263.2012.00372.x.

Bailey, J.J., Boyd, D.S., Hjort, J., Lavers, C.P., Field, R., 2017. Modelling native and alien vascular plant species richness: At which scales is geodiversity most relevant? Glob. Ecol. Biogeogr. 26, 763–776. https://doi.org/10.1111/geb.12574.

Balmford, A., 1996. Extinction filters and current resilience: the significance of past selection pressures for conservation biology. Trends Ecol. Evol. 11, 193–196. https://doi.org/10.1016/0169-5347(96)10026-4.

Barros, V.R., Boninsegna, J.A., Camilloni, I.A., Chidiak, M., Magrín, G.O., Rusticucci, M., 2015. Climate change in Argentina: trends, projections, impacts and adaptation. Wiley Interdiscip. Rev. Clim. Chang. 6, 151–169. https://doi.org/10.1002/wcc.316.

Barsi, J., Schott, J., Hook, S., Raqueno, N., Markham, B., Radocinski, R., 2014. Landsat-8 thermal infrared sensor (TIRS) vicarious radiometric calibration. Remote Sens. 6 (11), 11607–11626. https://doi.org/10.3390/rs61111607.

Behnke, R., Vavrus, S., Allstadt, A., Albright, T., Thogmartin, W.E., Radeloff, V.C., 2016. Evaluation of downscaled, gridded climate data for the conterminous United States. Ecol. Appl. 26, 1338–1351. https://doi.org/10.1002/15-1061.

Beller, E.E., Spotswood, E.N., Robinson, A.H., Anderson, M.G., Higgs, E.S., Hobbs, R.J., Suding, K.N., Zavaleta, E.S., Letitia Grenier, J., Grossinger, R.M., 2019. Building ecological resilience in highly modified landscapes. BioScience 69, 80–92. https://doi.org/10.1093/biosci/biy117.

Bellis, L.M., Pidgeon, A.M., Radeloff, V.C., St-Louis, V., Navarro, J.L., Martella, M.B., 2008. Modeling habitat suitability for greater rheas based on satellite image texture. Ecol. Appl. 18, 1956–1966. https://doi.org/10.1890/07-0243.1.

Beresford, A.E., Sanderson, F.J., Donald, P.F., Burfield, I.J., Butler, A., Vickery, J.A., Buchanan, G.M., 2019. Phenology and climate change in Africa and the decline of Afro-Palearctic migratory bird populations. Remote Sens. Ecol. Conserv. 5, 55–69. https://doi.org/10.1002/rse2.89.

Blundo, C., Gasparri, N.I., Malizia, A., Clark, M., Gatti, G., Campanello, P.I., Grau, H.R., Paolini, L., Malizia, L.R., Chediack, S.E., Macdonagh, P., Goldstein, G., 2018. Relationships among phenology, climate and biomass across subtropical forests in Argentina. J. Trop. Ecol. 34, 93–107. https://doi.org/10.1017/S026646741800010X.

Braatz, S., 2012. Building resilience for adaptation to climate change through sustainable forest management. Building resilience for adaptation to climate change in the agriculture sector. In: Proceedings of a Joint FAO/OECD Workshop 23–24 April 2012, pp. 117–127 doi:ISBN 978-92-5-107373-5.

Burkart, R., Bárbaro, N.O., Sánchez, R.O., Gómez, D.A., 1999. Ecorregiones de la Argentina. Buenos Aires Presidencia de la Nación Argentina. In: Buenos Aires Presidencia de la Nación Argentina, Secretaría de Recursos Naturales y Desarrollo Sustentable. Administración de Parques Nacionales, p. 72, 72 p.

Clarke, A., Gaston, K.J., 2006. Climate, energy and diversity. Proc. R. Soc. B Biol. Sci. 273, 2257–2266. https://doi.org/10.1098/rspb.2006.3545.

Colwell, R.K., Brehm, G., Cardelús, C.L., Gilman, A.C., Longino, J.T., Cardelus, C.L., Gilman, A.C., Longino, J.T., 2008. Global warming, elevational range shifts, and lowland biotic attrition in the wet tropics. Science 322, 258–261. https://doi.org/10.1126/science.1162547.

Culbert, P.D., Radeloff, V.C., St-Louis, V., Flather, C.H., Rittenhouse, C.D., Albright, T.P., Pidgeon, A.M., 2012. Modeling broad-scale patterns of avian species richness across the Midwestern United States with measures of satellite image texture. Remote Sens. Environ. 118, 140–150. https://doi.org/10.1016/j.rse.2011.11.004.

Currie, D.J., 2020. Energy and large-scale patterns of animal- and plant-species richness. Author (s): David J. Currie Source Am. Nat. 137 (1), 27–49 (Jan., 1991). Published by: The University of Chicago Press for The American Society 137, 27–49.

de Beurs, K.M., Henebry, G.M., 2004. Spatio-temporal statistical methods for modelling land surface phenology. In: Phenological Research: Methods for Environmental and Climate Change Analysis, pp. 177–208. https://doi.org/10.1007/978-90-481-3335-2.

de Beurs, K.M., Henebry, G.M., 2005. Land surface phenology and temperature variation in the International Geosphere-Biosphere Program high-latitude transects. Glob. Chang. Biol. 11, 779–790. https://doi.org/10.1111/j.1365-2486.2005.00949.x.

de Beurs, K.M., Henebry, G.M., 2010. Spatio-temporal statistical methods for modelling land surface phenology. In: Phenological Research. Springer Netherlands, pp. 177–207. https://doi.org/10.1007/978-90-481-3335-2.

Deng, G., Zhang, H., Guo, X., Shan, Y., Ying, H., Rihan, W., 2019. Asymmetric effects of daytime and nighttime warming on boreal forest spring phenology. Remote Sens. 11 https://doi.org/10.3390/rs11141651.

Elsen, P.R., Farwell, L.S., Pidgeon, A.M., Radeloff, V.C., 2020. Landsat 8 TIRS-derived relative temperature and thermal heterogeneity predict winter bird species richness patterns across the conterminous United States. Remote Sens. Environ. 236 https://doi.org/10.1016/j.rse.2019.111514.

Elsen, P.R., Farwell, L.S., Pidgeon, A.M., Radeloff, V.C., 2021. Contrasting seasonal patterns of relative temperature and thermal heterogeneity and their influence on breeding and winter bird richness patterns across the conterminous United States. Ecography 1–13. https://doi.org/10.1111/ecog.05520.

Fahrig, L., 2003. Effects of habitat fragmentation on biodiversity. Annu. Rev. Ecol. Evol. Syst. 34, 487–515. https://doi.org/10.1146/annurev.ecolsys.34.011802.132419.

Farwell, L.S., Elsen, P.R., Razenkova, E., Pidgeon, A.M., Radeloff, V.C., 2020. Habitat heterogeneity captured by 30-m resolution image texture predicts bird richness across the conterminous USA. Ecol. Appl. 30 https://doi.org/10.1002/eap.2157.

Farwell, L.S., Gudex-Cross, D., Anise, I.E., Bosch, M.J., Olah, A.M., Radeloff, V.C., Razenkova, E., Rogova, N., Silveira, E.M.O., Smith, M.M., Pidgeon, A.M., 2021. Satellite image texture captures vegetation heterogeneity and explains patterns of bird richness. Remote Sens. Environ. 253, 112175. https://doi.org/10.1016/j.rse.2020.112175.

Feit, B., Blüthgen, N., Traugott, M., Jonsson, M., 2019. Resilience of ecosystem processes: a new approach shows that functional redundancy of biological control services is reduced by landscape simplification. Ecol. Lett. 22, 1568–1577. https://doi.org/10.1111/ele.13347.

Ferrante, M., Barone, G., Kiss, M., Bozóné-Borbáth, E., Lövei, G.L., 2017. Ground-level predation on artificial caterpillars indicates no enemy-free time for lepidopteran larvae. Commun. Ecol. 18, 280–286. https://doi.org/10.1556/168.2017.18.3.6.

Ferrer-Paris, J.R., Zager, I., Keith, D.A., Oliveira-Miranda, M.A., Rodríguez, J.P., Josse, C., González-Gil, M., Miller, R.M., Zambrana-Torrelio, C., Barrow, E., 2019.

An ecosystem risk assessment of temperate and tropical forests of the Americas with an outlook on future conservation strategies. Conserv. Lett. 12, 1–10. https://doi.org/10.1111/conl.12623.
Fletcher, R.J., Didham, R.K., Banks-Leite, C., Barlow, J., Ewers, R.M., Rosindell, J., Holt, R.D., Gonzalez, A., Pardini, R., Damschen, E.I., Melo, F.P.L., Ries, L., Prevedello, J.A., Tscharntke, T., Laurance, W.F., Lovejoy, T., Haddad, N.M., 2018. Is habitat fragmentation good for biodiversity? Biol. Conserv. 226, 9–15. https://doi.org/10.1016/j.biocon.2018.07.022.
Folke, C., Carpenter, S., Walker, B., Scheffer, M., Elmqvist, T., Gunderson, L., Holling, C. S., 2004. Regime shifts, resilience, and biodiversity in ecosystem management. Annu. Rev. Ecol. Evol. Syst. 35, 557–581. https://doi.org/10.1146/annurev.ecolsys.35.021103.105711.
Galatowitsch, S., Frelich, L., Phillips-Mao, L., 2009. Regional climate change adaptation strategies for biodiversity conservation in a midcontinental region of North America. Biol. Conserv. 142, 2012–2022. https://doi.org/10.1016/j.biocon.2009.03.030.
Ganguly, S., Friedl, M.A., Tan, B., Zhang, X., Verma, M., 2010. Land surface phenology from MODIS: characterization of the collection 5 global land cover dynamics product. Remote Sens. Environ. 114, 1805–1816. https://doi.org/10.1016/j.rse.2010.04.005.
Garcia, R.A., Cabeza, M., Rahbek, C., Araújo, M.B., 2014. Multiple dimensions of climate change and their implications for biodiversity. Science 344. https://doi.org/10.1126/science.1247579.
García-álvarez, D., Van Delden, H., Teresa, M., Olmedo, C., Paegelow, M., 2019. Remote Sensing Technology for Evaluation of Variations in Land Surface Temperature, and Case Study Analysis from Southwest Nigeria: Volume Eight. Springer International Publishing. https://doi.org/10.1007/978-3-030-04750-4.
Ge, S., Carruthers, R., Gong, P., Herrera, A., 2006. Texture analysis for mapping *Tamarix parviflora* using aerial photographs along the Cache Creek, California. Environ. Monit. Assess. 114, 65–83. https://doi.org/10.1007/s10661-006-1071-z.
Getis, A., Ord, J.K., 1992. The analysis of spatial association. Geogr. Anal. 24, 189–206.
Gill, J.L., Blois, J.L., Benito, B., Dobrowski, S., Hunter, M.L., Mcguire, J.L., 2015. A 2.5-million-year perspective on coarse-filter strategies for conserving nature's stage. Conserv. Biol. 29, 640–648. https://doi.org/10.1111/cobi.12504.
Ginzburg, R., Adámoli, Y.J., 2006. Situacion ambiental en el Chaco Humedo. In: La Situacion Ambiental En El Chaco Humedo, pp. 103–113.
Glennon, M.J., Langdon, S.F., Rubenstein, M.A., Cross, M.S., 2019. Temporal changes in avian community composition in lowland conifer habitats at the southern edge of the boreal zone in the Adirondack Park, NY. PLoS One 14, 1–18. https://doi.org/10.1371/journal.pone.0220927.
González-Braojos, S., Sanz, J.J., Moreno, J., 2017. Decline of a montane Mediterranean pied flycatcher *Ficedula hypoleuca* population in relation to climate. J. Avian Biol. 48, 1383–1393. https://doi.org/10.1111/jav.01405.
Gray, M., 2008. Geodiversity: developing the paradigm. Proc. Geol. Assoc. 119, 287–298. https://doi.org/10.1016/S0016-7878(08)80307-0.
Hall-Beyer, M., 2003. Comparison of single-year and multiyear NDVI time series principal components in cold temperate biomes. IEEE Trans. Geosci. Remote Sens. 41, 2568–2574. https://doi.org/10.1109/TGRS.2003.817274.
Hansen, M.C., Potapov, P.V., Moore, R., Hancher, M., Turubanova, S.A., Tyukavina, A., Thau, D., Stehman, S.V., Goetz, S.J., Loveland, T.R., Kommareddy, A., Egorov, A., Chini, L., Justice, C.O., Townshend, J.R.G., 2013. High-resolution global maps of 21st-century forest cover change. Science 342, 850–853. https://doi.org/10.1126/science.1244693.
Haralick, R.M., Shanmugam, K., Dinstein, I., 1973. Textural features for image classification. IEEE Trans. Syst. Man Cybern. 3, 610–621.
Harrington, R., Woiwod, I., Sparks, T., 1999. Climate change and trophic interactions. Tree 14, 146–150.
Hengl, T., Heuvelink, G.B.M., Tadić, M.P., Pebesma, E.J., 2012. Spatio-temporal prediction of daily temperatures using time-series of MODIS LST images. Theor. Appl. Climatol. 107, 265–277. https://doi.org/10.1007/s00704-011-0464-2.
Hikosaka, K., Ishikawa, K., Borjigidai, A., Muller, O., Onoda, Y., 2006. Temperature acclimation of photosynthesis: mechanisms involved in the changes in temperature dependence of photosynthetic rate. J. Exp. Bot. 57, 291–302. https://doi.org/10.1093/jxb/erj049.
Hmielowski, T.L., Carter, S.K., Spaul, H., Helmers, D.P., Radeloff, V.C., Zedler, P.H., 2015. Prioritizing land management efforts at a landscape scale: a case study using prescribed fire in Wisconsin. Ecol. Appl. 26, 1018–1029. https://doi.org/10.1890/15-0509.1.
Hmimina, G., Dufrêne, E., Pontailler, J.Y., Delpierre, N., Aubinet, M., Caquet, B., de Grandcourt, A., Burban, B., Flechard, C., Granier, A., Gross, P., Heinesch, B., Longdoz, B., Moureaux, C., Ourcival, J.M., Rambal, S., Saint André, L., Soudani, K., 2013. Evaluation of the potential of MODIS satellite data to predict vegetation phenology in different biomes: an investigation using ground-based NDVI measurements. Remote Sens. Environ. 132, 145–158. https://doi.org/10.1016/j.rse.2013.01.010.
Holling, C.S., 1973. Resilience and stability of ecological systems. Annu. Rev. Ecol. Syst. 4, 1–23.
Hu, Q., Sulla-Menashe, D., Xu, B., Yin, H., Tang, H., Yang, P., Wu, W., 2019. A phenology-based spectral and temporal feature selection method for crop mapping from satellite time series. Int. J. Appl. Earth Obs. Geoinf. 80, 218–229. https://doi.org/10.1016/j.jag.2019.04.014.
Huete, A.R., Didan, K., Van Leeuwen, W., 1999. Modis Vegetation Index, Vol. 3. Vegetation Index and Phenology Lab, p. 129.
Huete, A., Didan, K., Miura, H., Rodriguez, E.P., Gao, X., Ferreira, L.F., 2002. Overview of the radiometric and biopyhsical performance of the MODIS vegetation indices. Remote Sens. Environ. 83, 195–213.
INTA, 2009. Monitoreo de la Cobertura y el Uso del Suelo a partir de sensores remotos. In: Informe Técnico Unificado PNECO 1643.
Jetz, W., McGeoch, M.A., Guralnick, R., Ferrier, S., Beck, J., Costello, M.J., Fernandez, M., Geller, G.N., Keil, P., Merow, C., Meyer, C., Muller-Karger, F.E., Pereira, H.M., Regan, E.C., Schmeller, D.S., Turak, E., 2019. Essential biodiversity variables for mapping and monitoring species populations. Nat. Ecol. Evol. 3, 539–551. https://doi.org/10.1038/s41559-019-0826-1.
Jin, H., Eklundh, L., 2014. A physically based vegetation index for improved monitoring of plant phenology. Remote Sens. Environ. 152, 512–525. https://doi.org/10.1016/j.rse.2014.07.010.
Jolliffe, I.T., Cadima, J., 2016. Principal component analysis: a review and recent developments. Philos. Trans. R. Soc. B Biol. Sci. 374, 1–16. https://doi.org/10.1098/rsta.2015.0202.
Jönsson, P., Eklundh, L., 2004. TIMESAT – a program for analyzing time-series of satellite sensor data. Comput. Geosci. 30, 833–845. https://doi.org/10.1016/j.cageo.2004.05.006.
Keppel, G., Van Niel, K.P., Wardell-Johnson, G.W., Yates, C.J., Byrne, M., Mucina, L., Schut, A.G.T., Hopper, S.D., Franklin, S.E., 2012. Refugia: Identifying and understanding safe havens for biodiversity under climate change. Glob. Ecol. Biogeogr. 21, 393–404. https://doi.org/10.1111/j.1466-8238.2011.00686.x.
Keppel, G., Mokany, K., Wardell-Johnson, G.W., Phillips, B.L., Welbergen, J.A., Reside, A.E., 2015. The capacity of refugia for conservation planning under climate change. Front. Ecol. Environ. 13, 106–112. https://doi.org/10.1890/140055Steinsdfdf.
Kerr, J.T., Packer, L., 1997. Habitat heterogeneity as a determinant of mammal species richness in high-energy regions. Nature 385, 252–254.
Koppen, W., Volken, E., Brönnimann, S., 2011. The thermal zones of the Earth according to the duration of hot, moderate and cold periods and to the impact of heat on the organic world. Meteorol. Z. 20, 351–360. https://doi.org/10.1127/0941-2948/2011/105.
Lawler, J.J., Ackerly, D.D., Albano, C.M., Anderson, M.G., Dobrowski, S.Z., Gill, J.L., Heller, N.E., Pressey, R.L., Sanderson, E.W., Weiss, S.B., 2015. The theory behind, and the challenges of, conserving nature's stage in a time of rapid change. Conserv. Biol. 29, 618–629. https://doi.org/10.1111/cobi.12505.
Letten, A.D., Ashcroft, M.B., Keith, D.A., Gollan, J.R., Ramp, D., 2013. The importance of temporal climate variability for spatial patterns in plant diversity. Ecography 36, 1341–1349. https://doi.org/10.1111/j.1600-0587.2013.00346.x.
Levin, N., Shmida, A., Levanoni, O., Tamari, H., Kark, S., 2007. Predicting mountain plant richness and rarity from space using satellite-derived vegetation indices. Divers. Distrib. 13, 692–703. https://doi.org/10.1111/j.1472-4642.2007.00372.x.
Liu, Y., Wu, C., Peng, D., Xu, S., Gonsamo, A., Jassal, R.S., Altaf Arain, M., Lu, L., Fang, B., Chen, J.M., 2016. Improved modeling of land surface phenology using MODIS land surface reflectance and temperature at evergreen needleleaf forests of central North America. Remote Sens. Environ. 176, 152–162. https://doi.org/10.1016/j.rse.2016.01.021.
Liu, H., Zhang, M., Lin, Z., Xu, X., 2018. Spatial heterogeneity of the relationship between vegetation dynamics and climate change and their driving forces at multiple time scales in Southwest China. Agric. For. Meteorol. 256–257, 10–21. https://doi.org/10.1016/j.agrformet.2018.02.015.
Lizárraga, L., Monguillot, J., 2020. Mapa de huella humana para Argentina. Diseño e implementación de un sistema de monitoreo en senderos. In: Boletín de Investigación y Monitoreo en Áreas Protegidas N°4. Dirección Regional Noroeste, Administración de Parques Nacionales, pp. 16–18. Pag.. Available at: https://sib.gob.ar/archivos/Boletin_IyM_DRNOA_4.pdf.
Loarie, S.R., Duffy, P.B., Hamilton, H., Asner, G.P., Field, C.B., Ackerly, D.D., 2009. The velocity of climate change. Nature 462, 1052–1055. https://doi.org/10.1038/nature08649.
Loreau, M., Naeem, S., Inchausti, P., Bengtsson, J., Grime, J.P., Hector, A., Hooper, D.U., Huston, M.A., Raffaelli, D., Schmid, B., Tilman, D., Wardle, D.A., 2001. Ecology: biodiversity and ecosystem functioning: current knowledge and future challenges. Science 294, 804–808. https://doi.org/10.1126/science.1064088.
Loveland, T.R., Merchant, J.M., 2004. Ecoregions and ecoregionalization: geographical and ecological perspectives. Environ. Manag. 34 (Suppl. 1), 1–13. https://doi.org/10.1007/s00267-003-5181-x.
Lu, D., Batistella, M., 2005. Exploring TM image texture and its relationships with biomass estimation in Rondônia, Brazilian Amazon. Acta Amazon. 35, 249–257. https://doi.org/10.1590/S0044-59672005000200015.
Lu, L., Zhang, T., Wang, T., Zhou, X., 2018. Evaluation of collection-6 MODIS land surface temperature product using multi-year ground measurements in an arid area of northwest China. Remote Sens. 10 https://doi.org/10.3390/rs10111852.
Ma, X., Huete, A., Yu, Q., Coupe, N.R., Davies, K., Broich, M., Ratana, P., Beringer, J., Hutley, L.B., Cleverly, J., Boulain, N., Eamus, D., 2013. Spatial patterns and temporal dynamics in savanna vegetation phenology across the north australian tropical transect. Remote Sens. Environ. 139, 97–115. https://doi.org/10.1016/j.rse.2013.07.030.
MacArthur, R.H., 1972. Geographical Ecology. Patterns in the Distribution of Species. Harper and Row, New York, New York, USA. https://doi.org/10.1086/408050.
Malika, V.S., Lindsey, G., Katherine, J.W., 2009. How does spatial heterogeneity influence resilience to climatic changes? Ecological dynamics in southeast Madagascar. Ecol. Monogr. 79, 557–574. https://doi.org/10.1890/08-1210.1.
Mann, M.E., Park, J., 1996. Greenhouse warming and changes in the seasonal cycle of temperature: model versus observatons. Geophys. Res. Lett. 23 https://doi.org/10.1029/96GL01066.
Martin, C.E., Chehébar, C., 2001. The national parks of Argentinian Patagonia — management policies for conservation, public use, rural settlements, and indigenous

communities. J. R. Soc. N. Z. 31, 845–864. https://doi.org/10.1080/03014223.2001.9517680.
Martinuzzi, S., Rivera, L., Politi, N., Bateman, B.L., De Los Llanos, E.R., Lizarraga, L., Soledad De Bustos, M., Chalukian, S., Pidgeon, A.M., Radeloff, V.C., 2018. Enhancing biodiversity conservation in existing land-use plans with widely available datasets and spatial analysis techniques. Environ. Conserv. 45, 252–260. https://doi.org/10.1017/S0376892917000455.
Matsushita, B., Yang, W., Chen, J., Onda, Y., Qiu, G., 2007. Sensitivity of the Enhanced Vegetation Index (EVI) and Normalized Difference Vegetation Index (NDVI) to topographic effects: a case study in high-density cypress forest. Sensors 7, 2636–2651. https://doi.org/10.3390/s7112636.
Menzel, A., Sparks, T.H., Estrella, N., Roy, D.B., 2006. Altered geographic and temporal variability in phenology in response to climate change. Glob. Ecol. Biogeogr. 15, 498–504. https://doi.org/10.1111/j.1466-822X.2006.00247.x.
Miller-Rushing, A.J., Høye, T.T., Inouye, D.W., Post, E., 2010. The effects of phenological mismatches on demography. Philos. Trans. R. Soc. B Biol. Sci. 365, 3177–3186. https://doi.org/10.1098/rstb.2010.0148.
Misra, G., Buras, A., Heurich, M., Asam, S., Menzel, A., 2018. LiDAR derived topography and forest stand characteristics largely explain the spatial variability observed in MODIS land surface phenology. Remote Sens. Environ. 218, 231–244. https://doi.org/10.1016/j.rse.2018.09.027.
Morisette, J.T., Richardson, A.D., Knapp, A.K., Fisher, J.I., Graham, E.A., Abatzoglou, J., Wilson, B.E., Breshears, D.D., Henebry, G.M., Hanes, J.M., Liang, L., 2009. Tracking the rhythm of the seasons in the face of global change: phenological research in the 21 st century. Front. Ecol. Environ. 7, 253–260. https://doi.org/10.1890/070217.
Neiff, J.J., 2001. Diversity in some tropical wetland systems of South America. In: Biodiversity in Wetlands: Assessment, Function and Conservation, Vol. 2, pp. 157–186.
Nyström, M., Folke, C., 2001. Spatial resilience of coral reefs. Ecosystems 4, 406–417. https://doi.org/10.1007/s10021-001-0019-y.
Oliver, T., Roy, D.B., Hill, J.K., Brereton, T., Thomas, C.D., 2010. Heterogeneous landscapes promote population stability. Ecol. Lett. 13, 473–484. https://doi.org/10.1111/j.1461-0248.2010.01441.x.
Oliver, T.H., Heard, M.S., Isaac, N.J.B., Roy, D.B., Procter, D., Eigenbrod, F., Freckleton, R., Hector, A., Orme, C.D.L., Petchey, O.L., Proença, V., Raffaelli, D., Suttle, K.B., Mace, G.M., Martín-López, B., Woodcock, B.A., Bullock, J.M., 2015. Biodiversity and resilience of ecosystem functions. Trends Ecol. Evol. 30, 673–684. https://doi.org/10.1016/j.tree.2015.08.009.
Pearce-Higgins, J.W., Eglington, S.M., Martay, B., Chamberlain, D.E., 2015. Drivers of climate change impacts on bird communities. J. Anim. Ecol. 84, 943–954. https://doi.org/10.1111/1365-2656.12364.
Pereira, H.M., Leadley, P.W., Proença, V., Alkemade, R., Scharlemann, J.P.W., Fernandez-Manjarrés, J.F., Araújo, M.B., Balvanera, P., Biggs, R., Cheung, W.W.L., Chini, L., Cooper, H.D., Gilman, E.L., Guénette, S., Hurtt, G.C., Huntington, H.P., Mace, G.M., Oberdorff, T., Revenga, C., Rodrigues, P., Scholes, R.J., Sumaila, U.R., Walpole, M., 2010. Scenarios for global biodiversity in the 21st century. Science 330, 1496–1501. https://doi.org/10.1126/science.1196624.
Peterson, G., Allen, C.R., Holling, C.S., 1998. Ecological resilience, biodiversity, and scale. Ecosystems 1, 6–18.
Piha, H., Luoto, M., Piha, M., Merilä, J., 2007. Anuran abundance and persistence in agricultural landscapes during a climatic extreme. Glob. Chang. Biol. 13, 300–311. https://doi.org/10.1111/j.1365-2486.2006.01276.x.
Plard, F., Gaillard, J.M., Coulson, T., Hewison, A.J.M., Delorme, D., Warnant, C., Bonenfant, C., 2014. Mismatch between birth date and vegetation phenology slows the demography of roe deer. PLoS Biol. 12, 1–8. https://doi.org/10.1371/journal.pbio.1001828.
Possingham, H.P., Wilson, K.a, Andelman, S.J., Vynne, C.H., Vynme, C.H., 2006. Protected areas: goals, limitations, and design. Princ. Conserv. Biol. 509–551. https://doi.org/10.1023/A:1006601319528.
Read, Q.D., Zarnetske, P.L., Record, S., Dahlin, K.M., Costanza, J.K., Finley, A.O., Gaddis, K.D., Grady, J.M., Hobi, M.L., Latimer, A.M., Malone, S.L., Ollinger, S.V., Pau, S., Wilson, A.M., 2020. Beyond counts and averages: relating geodiversity to dimensions of biodiversity. Glob. Ecol. Biogeogr. 29, 696–710. https://doi.org/10.1111/geb.13061.
Reed, T.E., Grotan, V., Jenouvrier, S., Saether, B., Visser, M.E., 2013. Population growth in a wild bird is buffered against phenological mismatch. Science 340, 488–491. https://doi.org/10.1126/science.1232870.
Ren, J., Campbell, J.B., Shao, Y., 2017. Estimation of SOS and EOS for Midwestern US corn and soybean crops. Remote Sens. 9, 722. https://doi.org/10.3390/rs9070722.
Renner, S.S., Zohner, C.M., 2018. Climate change and phenological mismatch in trophic interactions among plants, insects, and vertebrates. Annu. Rev. Ecol. Evol. Syst. 49, 165–182. https://doi.org/10.1146/annurev-ecolsys-110617-062535.
Robinson, N.M., Leonard, S.W.J., Bennett, A.F., Clarke, M.F., 2016. Are forest gullies refuges for birds when burnt? The value of topographical heterogeneity to avian diversity in a fire-prone landscape. Biol. Conserv. 200, 1–7. https://doi.org/10.1016/j.biocon.2016.05.010.
Rosas, Y.M., Peri, P.L., Huertas Herrera, A., Pastore, H., Martínez Pastur, G., 2017. Modeling of potential habitat suitability of Hippocamelus bisulcus: effectiveness of a protected areas network in Southern Patagonia. Ecol. Process. 6. https://doi.org/10.1186/s13717-017-0096-2.
Rosas, Y.M., Peri, P.L., Bahamonde, H.A., Cellini, J.M., Barrera, M.D., Huertas Fereira, A., Lencinas, M.V., Martinez Pastur, G., 2019. Trade-Offs Between Management and Conservation for the Provision of Ecosystem Services in the Southern Patagonian Forests. Ed. J Stanturf, Cambridge, UK.
Saino, N., Ambrosini, R., Rubolini, D., Von Hardenberg, J., Provenzale, A., Hüppop, K., Hüppop, O., Lehikoinen, A., Lehikoinen, E., Rainio, K., Romano, M., Sokolov, L., 2011. Climate warming, ecological mismatch at arrival and population decline in migratory birds. Proc. R. Soc. B Biol. Sci. 278, 835–842. https://doi.org/10.1098/rspb.2010.1778.
Savitzky, A., Golay, M.J.E., 1964. Smoothing and differentiation of data by simplified least squares procedures. Anal. Chem. 36, 1627–1639. https://doi.org/10.1021/ac60214a047.
Scheffers, B.R., Edwards, D.P., Diesmos, A., Williams, S.E., Evans, T.A., 2014. Microhabitats reduce animal's exposure to climate extremes. Glob. Chang. Biol. 20, 495–503. https://doi.org/10.1111/gcb.12439.
Schwartz, M.D., Ahas, R., Aasa, A., 2006. Onset of spring starting earlier across the Northern Hemisphere. Glob. Chang. Biol. 12, 343–351. https://doi.org/10.1111/j.1365-2486.2005.01097.x.
Schweiger, O., Settele, J., Kudrna, O., Klotz, S., Kühn, I., 2008. Climate change can cause spatial mismatch of trophically interacting species. Ecology 89, 3472–3479. https://doi.org/10.1890/07-1748.1.
Seghezzo, L., Volante, J.N., Paruelo, J.M., Somma, D.J., Buliubasich, E.C., Rodríguez, H. E., Gagnon, S., Hufty, M., 2011. Native forests and agriculture in Salta (Argentina): conflicting visions of development. J. Environ. Dev. 20, 251–277. https://doi.org/10.1177/1070496511416915.
Sica, Y.V., Gavier-Pizarro, G.I., Pidgeon, A.M., Travaini, A., Bustamante, J., Radeloff, V. C., Quintana, R.D., 2018. Changes in bird assemblages in a wetland ecosystem after 14 years of intensified cattle farming. Aust. Ecol. 43, 786–797. https://doi.org/10.1111/aec.12621.
Sims, D.A., Rahman, A.F., Cordova, V.D., El-Masri, B.Z., Baldocchi, D.D., Flanagan, L.B., Goldstein, A.H., Hollinger, D.Y., Misson, L., Monson, R.K., Oechel, W.C., Schmid, H. P., Wofsy, S.C., Xu, L., 2006. On the use of MODIS EVI to assess gross primary productivity of North American ecosystems. J. Geophys. Res. Biogeosci. 111, 1–16. https://doi.org/10.1029/2006JG000162.
Socolar, J.B., Epanchin, P.N., Beissinger, S.R., Tingley, M.W., 2017. Phenological shifts conserve thermal niches in North American birds and reshape expectations for climate-driven range shifts. Proc. Natl. Acad. Sci. U. S. A. 114, 12976–12981. https://doi.org/10.1073/pnas.1705897114.
Srinivasan, U., Elsen, P.R., Wilcove, D.S., 2019. Annual temperature variation influences the vulnerability of montane bird communities to land-use change. Ecography 42, 2084–2094. https://doi.org/10.1111/ecog.04611.
Stein, A., Gerstner, K., Kreft, H., 2014. Environmental heterogeneity as a universal driver of species richness across taxa, biomes and spatial scales. Ecol. Lett. 17, 866–880. https://doi.org/10.1111/ele.12277.
St-Louis, V., Pidgeon, A.M., Radeloff, V.C., Hawbaker, T.J., Clayton, M.K., 2006. High-resolution image texture as a predictor of bird species richness. Remote Sens. Environ. 105, 299–312. https://doi.org/10.1016/j.rse.2006.07.003.
St-Louis, V., Pidgeon, A.M., Clayton, M.K., Locke, B.A., Bash, D., Radeloff, V.C., 2009. Satellite image texture and a vegetation index predict avian biodiversity in the Chihuahuan Desert of New Mexico. Ecography 32, 468–480. https://doi.org/10.1111/j.1600-0587.2008.05512.x.
Tews, J., Brose, U., Grimm, V., Tielbörger, K., Wichmann, M.C., Schwager, M., Jeltsch, F., 2004. Animal species diversity driven by habitat heterogeneity/diversity: the importance of keystone structures. J. Biogeogr. 31, 79–92. https://doi.org/10.1046/j.0305-0270.2003.00994.x.
Thackeray, S.J., Sparks, T.H., Frederiksen, M., Burthe, S., Bacon, P.J., Bell, J.R., Botham, M.S., Brereton, T.M., Bright, P.W., Carvalho, L., Clutton-Brock, T., Dawson, A., Edwards, M., Elliott, J.M., Harrington, R., Johns, D., Jones, I.D., Jones, J.T., Leech, D.I., Roy, D.B., Scott, W.A., Smith, M., Smithers, R.J., Winfield, I. J., Wanless, S., 2010. Trophic level asynchrony in rates of phenological change for marine, freshwater and terrestrial environments. Glob. Chang. Biol. 16, 3304–3313. https://doi.org/10.1111/j.1365-2486.2010.02165.x.
Thorpe, R.S., Surget-Groba, Y., Johansson, H., 2008. The relative importance of ecology and geographic isolation for speciation in anoles. Philos. Trans. R. Soc. B Biol. Sci. 363, 3071–3081. https://doi.org/10.1098/rstb.2008.0077.
Thuiller, W., Lavorel, S., Araújo, M.B., Sykes, M.T., Prentice, I.C., 2005. Climate change threats to plant diversity in Europe. Proc. Natl. Acad. Sci. U. S. A. 102, 8245–8250. https://doi.org/10.1073/pnas.0409902102.
Tilman, D., 1999. The ecological consequences of changes in biodiversity: a search for general principles. Ecology 80, 1455–1474. https://doi.org/10.2307/176540.
Tingley, M.W., Darling, E.S., Wilcove, D.S., 2014. Fine- and coarse-filter conservation strategies in a time of climate change. Ann. N. Y. Acad. Sci. 1322, 92–109. https://doi.org/10.1111/nyas.12484.
Turner, M.G., Donato, D.C., Romme, W.H., 2013. Consequences of spatial heterogeneity for ecosystem services in changing forest landscapes: priorities for future research. Landsc. Ecol. 28, 1081–1097. https://doi.org/10.1007/s10980-012-9741-4.
UNEP-WCMC, 2020. Protected Area Profile for Argentina from the World Database of Protected Areas, April 2020. Available at: www.protectedplanet.net.
Van Leeuwen, W.J.D., Hartfield, K., Miranda, M., Meza, F.J., 2013. Trends and ENSO/AAO driven variability in NDVI derived productivity and phenology alongside the Andes Mountains. Remote Sens. 5, 1177–1203. https://doi.org/10.3390/rs5031177.
Vejsbjerg, L., Nunez, P., Matossian, B., 2014. Transformation of frontier National Parks into tourism sites: the North Andean Patagonia experience (1934-1955). J. Tour. Cult. Territorial Dev. 10, 1–22.
Venter, O., Fuller, R.A., Segan, D.B., Carwardine, J., Brooks, T., Butchart, S.H.M., Di Marco, M., Iwamura, T., Joseph, L., O'Grady, D., Possingham, H.P., Rondinini, C., Smith, R.J., Venter, M., Watson, J.E.M., 2014. Targeting global protected area expansion for imperiled biodiversity. PLoS Biol. 12. https://doi.org/10.1371/journal.pbio.1001891.
Vina, A., Gitelson, A.A., Rundquist, D.C., Keydan, G., Leavitt, B., Schepers, J., 2004. Monitoring maize (*Zea mays* L.) phenology with remote sensing. Remote Sens. 1147, 1139–1147.

Virah-sawmy, M., Gillson, L., Willis, K.J., 2009. How does spatial heterogeneity influence resilience to climatic changes? Ecol. Monogr. 79, 557–574.
Waldock, C., Dornelas, M., Bates, A.E., 2018. Temperature-driven biodiversity change: disentangling space and time. BioScience 68, 873–884. https://doi.org/10.1093/biosci/biy096.
Wang, J., Meng, J.J., Cai, Y.L., 2008. Assessing vegetation dynamics impacted by climate change in the southwestern karst region of China with AVHRR NDVI and AVHRR NPP time-series. Environ. Geol. 54, 1185–1195. https://doi.org/10.1007/s00254-007-0901-9.
Wardlow, B.D., Kastens, J.H., Egbert, S.L., 2006. Using USDA crop progress data for the evaluation of greenup onset date calculated from MODIS 250-meter data. Photogramm. Eng. Remote. Sens. 72, 1225–1234.
White, M.A., Nemani, R.R., 2006. Real-time monitoring and short-term forecasting of land surface phenology. Remote Sens. Environ. 104, 43–49. https://doi.org/10.1016/j.rse.2006.04.014.
White, M.A., de Beurs, K.M., Didan, K., Inouye, D.W., Richardson, A.D., Jensen, O.P., O'Keefe, J., Zhang, G., Nemani, R.R., van Leeuwen, W.J.D., Brown, J.F., de Wit, A., Schaepman, M., Lin, X., Dettinger, M., Bailey, A.S., Kimball, J., Schwartz, M.D., Baldocchi, D.D., Lee, J.T., Lauenroth, W.K., 2009. Intercomparison, interpretation, and assessment of spring phenology in North America estimated from remote sensing for 1982-2006. Glob. Chang. Biol. 15, 2335–2359. https://doi.org/10.1111/j.1365-2486.2009.01910.x.
Wilson, K.A., McBride, M.F., Bode, M., Possingham, H.P., 2006. Prioritizing global conservation efforts. Nature 440, 337–340. https://doi.org/10.1038/nature04366.
Wood, E.M., Pidgeon, A.M., Radeloff, V.C., Keuler, N.S., 2012. Image texture as a remotely sensed measure of vegetation structure. Remote Sens. Environ. 121, 516–526. https://doi.org/10.1016/j.rse.2012.01.003.
Wood, E.M., Pidgeon, A.M., Radeloff, V.C., Keuler, N.S., 2013. Image texture predicts avian density and species richness. PLoS One 8. https://doi.org/10.1371/journal.pone.0063211.
Wu, C., Gonsamo, A., Gough, C.M., Chen, J.M., Xu, S., 2014. Modeling growing season phenology in North American forests using seasonal mean vegetation indices from MODIS. Remote Sens. Environ. 147, 79–88. https://doi.org/10.1016/j.rse.2014.03.001.
Wulder, M.A., LeDrew, E.F., Franklin, S.E., Lavigne, M.B., 1998. Aerial image texture information in the estimation of northern deciduous and mixed wood forest leaf area index (LAI). Remote Sens. Environ. 64, 64–76. https://doi.org/10.1016/S0034-4257(97)00169-7.
Xia, H., Qin, Y., Feng, G., Meng, Q., Cui, Y., Song, H., Ouyang, Y., Liu, G., 2019. Forest phenology dynamics to climate change and topography in a geographic and climate transition zone: the Qinling Mountains in Central China. Forests 10, 1–24. https://doi.org/10.3390/f10111007.
Zarnetske, P.L., Read, Q.D., Record, S., Gaddis, K.D., Pau, S., Hobi, M.L., Malone, S.L., Costanza, J., Dahlin, K.M., Latimer, A.M., Wilson, A.M., Grady, J.M., Ollinger, S.V., Finley, A.O., 2019. Towards connecting biodiversity and geodiversity across scales with satellite remote sensing. Glob. Ecol. Biogeogr. 28, 548–556. https://doi.org/10.1111/geb.12887.
Zeng, L., Wardlow, B.D., Xiang, D., Hu, S., Li, D., 2020. A review of vegetation phenological metrics extraction using time-series, multispectral satellite data. Remote Sens. Environ. 237, 111511. https://doi.org/10.1016/j.rse.2019.111511.
Zhang, X., Wang, J., Gao, F., Liu, Y., Schaaf, C., Friedl, M., Yu, Y., Jayavelu, S., Gray, J., Liu, L., Yan, D., Henebry, G.M., 2017. Exploration of scaling effects on coarse resolution land surface phenology. Remote Sens. Environ. 190, 318–330. https://doi.org/10.1016/j.rse.2017.01.001.
Zhang, Y., Loreau, M., He, N., Wang, J., Pan, Q., Bai, Y., Han, X., 2018. Climate variability decreases species richness and community stability in a temperate grassland. Oecologia 188, 183–192. https://doi.org/10.1007/s00442-018-4208-1.